



**UNIVERSIDADE ESTADUAL DE CAMPINAS
FACULDADE DE ENGENHARIA QUÍMICA**

ISA SILVEIRA DE ARAÚJO

**MODELING OF MIXTURE ADSORPTION: AN EXTENSION OF SAFT-VR MIE
EQUATION OF STATE**

**MODELAGEM DE ADSORÇÃO DE MISTURAS: UMA EXTENSÃO DA EQUAÇÃO DE
ESTADO SAFT-VR MIE**

CAMPINAS

2019

ISA SILVEIRA DE ARAÚJO

MODELING OF MIXTURE ADSORPTION: AN EXTENSION OF SAFT-VR MIE
EQUATION OF STATE

MODELAGEM DE ADSORÇÃO DE MISTURAS: UMA EXTENSÃO DA EQUAÇÃO DE
ESTADO SAFT-VR MIE

Dissertation presented to the School of Chemical Engineering of the University of Campinas in partial fulfillment of the requirements for the degree of Master in Chemical Engineering.

Dissertação apresentada à Faculdade de Engenharia Química da Universidade Estadual de Campinas como parte dos requisitos exigidos para a obtenção do título de Mestre em Engenharia Química.

Orientador: Prof. Dr. Luís Fernando Mercier Franco

ESTE EXEMPLAR CORRESPONDE À VERSÃO FINAL DA DISSERTAÇÃO DEFENDIDA PELA ALUNA ISA SILVEIRA DE ARAÚJO E ORIENTADA PELO PROF. DR. LUÍS FERNANDO MERCIER FRANCO.

CAMPINAS/SP

2019

Ficha catalográfica
Universidade Estadual de Campinas
Biblioteca da Área de Engenharia e Arquitetura
Luciana Pietrosanto Milla - CRB 8/8129

Ar12m Araújo, Isa Silveira de, 1992-
Modeling of mixture adsorption: an extension of SAFT-VR Mie equation of state / Isa Silveira de Araújo. – Campinas, SP : [s.n.], 2019.

Orientador: Luís Fernando Mercier Franco.
Dissertação (mestrado) – Universidade Estadual de Campinas, Faculdade de Engenharia Química.

1. Adsorção. 2. Mistura. 3. Equação de estado. I. Franco, Luís Fernando Mercier, 1988-. II. Universidade Estadual de Campinas. Faculdade de Engenharia Química. III. Título.

Informações para Biblioteca Digital

Título em outro idioma: Modelagem de adsorção de misturas: uma extensão da equação de estado SAFT-VR Mie

Palavras-chave em inglês:

Adsorption

Mixture

Equation of state

Área de concentração: Engenharia Química

Titulação: Mestra em Engenharia Química

Banca examinadora:

Luís Fernando Mercier Franco [Orientador]

Roger Josef Zemp

Frederico Wanderley Tavares

Data de defesa: 09-05-2019

Programa de Pós-Graduação: Engenharia Química

Identificação e informações acadêmicas do(a) aluno(a)

- ORCID do autor: <https://orcid.org/0000-0002-0203-2896>

- Currículo Lattes do autor: <http://lattes.cnpq.br/2418292436702255>

FOLHA DE APROVAÇÃO

Folha de Aprovação da Dissertação de Mestrado defendida por Isa Silveira de Araújo e aprovada em 09 de maio de 2019 pela banca examinadora constituída pelos seguintes doutores

Prof. Dr. Luís Fernando Mercier Franco - Orientador

FEQ - UNICAMP

Prof. Dr. Roger Josef Zemp

FEQ/UNICAMP

Dr. Frederico Wanderley Tavares

UFRJ/Escola de Química

ATA da Defesa com as respectivas assinaturas dos membros encontra-se no SIGA/Sistema de Fluxo de Dissertação/Tese e na Secretaria do Programa da Unidade.

"Desde os tempos antigos ninguém ouviu, nenhum ouvido percebeu, e olho nenhum viu outro Deus, além de ti, que trabalha para aqueles que nele esperam."

Isaías 64:4

Acknowledgements

Agradeço a Deus, minha fonte de força e fé para nunca desistir e alcançar meus objetivos.

Aos meus pais, Herbet e Ircemes, irmã, Ivine, pelas orações e por não medirem esforços para ajudar a conquistar meus sonhos.

Ao meu noivo, Kíldare, pela paciência, carinho e sábias palavras de encorajamento que foram tão importantes nessa trajetória.

Ao meu orientador, Luís Fernando Mercier Franco, que com todo o seu conhecimento e entusiasmo pela ciência, mudou a minha forma de ver a Engenharia Química. Muito obrigada pela confiança, amizade e paciência, para mim foi uma honra tê-lo como orientador.

A todos que fazem parte do LESC, especialmente Joyce, Marcelle e Rodrigo, vocês foram minha família em Campinas. Obrigada pelo carinho, pelos momentos de muita risada, pelas palavras de força e pelas constantes ajudas no meu projeto. Sem vocês, esse período não teria sido tão bom.

À minha amiga Alexandra, obrigada pela parceria, pelas palavras de ânimo, pelas orações e sábios conselhos.

À CAPES: O presente trabalho foi realizado com apoio da Coordenação de Aperfeiçoamento de Pessoal de Nível Superior-Brazil (CAPES) código de Financiamento 001.

Agradeço também ao CENAPAD pelo suporte computacional.

Por fim, a todos aqueles que contribuíram, direta ou indiretamente, para a realização desta dissertação, o meu sincero agradecimento.

Resumo

Os fluidos confinados representam uma área de estudo ampla e que tem chamado muita atenção por ser um sistema muito comum nas atividades práticas da engenharia. Apesar de sua aplicabilidade, ainda é considerado um campo de estudo complexo e incipiente. Isto está relacionado a fatores que podem modificar as propriedades dos fluidos confinados, dentre eles: a geometria, tamanho do poro, e as interações entre a parede e o fluido. No que diz respeito às ferramentas utilizadas para descrição destes sistemas, simulação molecular, teoria do funcional da densidade e equações de estados são as mais exploradas. Porém, as equações de estado ainda permanecem como a abordagem mais versátil e menos custosa em termos computacionais. Neste trabalho, a equação de estado *Statistical Associating Fluid Theory* (SAFT-VR Mie) foi adaptada para calcular isotermas de adsorção de misturas. Um termo que descreve a energia de Helmholtz devido aos efeitos de confinamento foi acoplado à equação de estado SAFT-VR Mie. O desenvolvimento teórico deste termo é baseado na teoria generalizada de van der Waals, e a interação fluido parede é modelada pelo potencial de poço quadrado. A estrutura do fluido consequente das interações entre a superfície e o fluido foi derivada utilizando o teorema do valor médio. O modelo resultante leva em conta a geometria, tamanho do poro e depende apenas dos parâmetros de interação entre o fluido e a parede. Estes parâmetros foram calculados através de regras de combinação dos parâmetros de interação dos fluidos puros, o que faz o modelo totalmente preditivo. Para resolver o critério de equilíbrio de fases, o método da secante multidimensional foi utilizado, e isotermas de adsorção de multicomponentes foram obtidas para diferentes sistemas. Para verificar a consistência do modelo, as isotermas de misturas calculadas foram comparadas com dados experimentais retirados da literatura, e bons resultados foram obtidos.

Palavras-chaves: SAFT-VR Mie, Adsorção, Fluidos Confinados, Mistura

Abstract

Confined fluid systems consist of a broad subject that draws remarkable attention being so common in engineering. Despite its applicability, it is still considered an incipient and complex field of study. This is related to the many factors that can modify the properties of confined fluids, for example: pore size and geometry distribution of the confining material, and the interactions between the wall and fluid. Regarding the tools used to describe these systems, molecular simulation, Density Functional Theory (DFT), and Equation of State (EoS) are the most explored ones. The latter, however, remains as the most versatile and the least computational demanding approach. In this work, we extend the Statistical Associating Fluid Theory (SAFT-VR Mie) equation of state for the calculation of multicomponent adsorption isotherms. A term that describes the Helmholtz free energy due to confinement effect is coupled with the SAFT-VR Mie equation of state. The theoretical development of this term is based on the generalized van der Waals framework, and the fluid-wall interactions are modeled as a square-well potential. The fluid structure resulting from the interactions between surface and fluid are derived by applying the mean value theorem. The resulting model takes into account the geometry and size of the pore, and depends solely on the wall-fluid interaction parameters. The required mixture wall-fluid interaction parameters were calculated by applying combining rules to the pure component interaction parameters, bringing to the model a predictive feature. To solve the phase equilibrium criteria, the multidimensional secant method was employed, and multicomponent adsorption isotherms were predicted for different systems. To verify the consistency of the model, the calculated multicomponent isotherms were compared to experimental data reported in the literature and reasonably accurate results were obtained.

Keywords: SAFT-VR Mie, Adsorption, Confined Fluids, Mixture

List of Figures

Figure 1	– The six types of isotherm (IUPAC classification) (KELLER; STAUDT, 2005)	24
Figure 2	– Regions inside a pore for a fluid that interacts via square-well potential . . .	37
Figure 3	– Snapshot of a Monte Carlo simulation for a binary system.	41
Figure 4	– Radial distribution functions for a mixture with composition 25% – 75%: Blue line is the radial distribution function for the pure component with $\sigma = 1$, red line is the pure component with $\sigma = 2$ and the green line is the radial distribution function for mixture. The range of attraction λ was set to 1.5 for each component	42
Figure 5	– Radial distribution function at contact for different compositions: blue line = 40%-60%; black line = 25%-75%; green line = 20%-80%; red line = 10%-90%	43
Figure 6	– ξ_{12} as function of ζ_3 for different square-well binary mixtures (25% of molecules type 1 and 75% of molecules type 2): i) $\lambda_{11} = 1.1$, $\lambda_{22} = 1.3$, and $\lambda_{12} = 1.2$ (yellow); ii) $\lambda_{11} = 1.125$, $\lambda_{22} = 1.500$, and $\lambda_{12} = 1.313$ (red); iii) and $\lambda_{11} = 1.375$, $\lambda_{22} = 1.625$, and $\lambda_{12} = 1.500$ (blue); Closed symbols, Monte Carlo simulations. Continuous lines, Equations (4.28) and (4.29). . .	44
Figure 7	– Adsorption isotherms of methane and ethane on a carbon molecular sieve (MSC5A) at 303.15 K with bulk pressure of 13.3 kPa. Closed symbols, experimental data (KONNO; SHIBATA; SAITO, 1985). Continuous lines, proposed model.	49
Figure 8	– Adsorption isotherms of methane and ethane on a carbon molecular sieve (MSC5A) at 303.15 K with bulk pressure of 40.0 kPa. Closed symbols, experimental data (KONNO; SHIBATA; SAITO, 1985). Continuous lines, proposed model.	50
Figure 9	– Adsorption isotherms of ethane and propane on a carbon molecular sieve (MSC5A) at 303.15 K with bulk pressure of 13.3 kPa. Closed symbols, experimental data (KONNO; SHIBATA; SAITO, 1985). Continuous lines, proposed model.	50

Figure 10 – Adsorption isotherms of ethane and propane on a carbon molecular sieve (MSC5A) at 303.15 K with bulk pressure of 40.0 kPa. Closed symbols, experimental data (KONNO; SHIBATA; SAITO, 1985). Continuous lines, proposed model.	51
Figure 11 – Adsorption isotherms of ethylene and propane on a carbon molecular sieve (MSC5A) at 303.15 K with bulk pressure of 13.3 kPa. Closed symbols, experimental data (KONNO; SHIBATA; SAITO, 1985). Continuous lines, proposed model.	51
Figure 12 – Adsorption isotherms of methane and nitrogen on a MOF-5 at 297.0 K with bulk pressure of 502.0 kPa. Closed symbols, experimental data (KLOUTSE et al., 2018). Continuous lines, proposed model.	53
Figure 13 – Adsorption isotherms of methane and nitrogen on a MOF-5 at 297.0 K with bulk pressure of 1506.0 kPa. Closed symbols, experimental data (KLOUTSE et al., 2018). Continuous lines, proposed model.	54
Figure 14 – Adsorption isotherm for pure methane on MOF-5 at 297 K Closed symbols, experimental data (KLOUTSE et al., 2018). Continuous lines, proposed model.	54
Figure 15 – Adsorption isotherm for pure nitrogen on MOF-5 at 297 K Closed symbols, experimental data (KLOUTSE et al., 2018). Continuous lines, proposed model.	55
Figure 16 – Adsorption isotherm for pure hydrogen on activated carbon JX101 at 298 K Closed symbols, experimental data (WU et al., 2005). Continuous lines, proposed model.	55
Figure 17 – Adsorption isotherm for pure hydrogen on activated carbon JX101 at 313 K Closed symbols, experimental data (WU et al., 2005). Continuous lines, proposed model.	56
Figure 18 – Adsorption isotherm for the ternary mixture of methane, nitrogen, and hydrogen on activated carbon JX101 at 298 K with bulk mole fractions of 0.3648, 0.2775, and 0.3577, respectively. Closed symbols, experimental data (WU et al., 2005). Continuous lines, proposed model.	57
Figure 19 – Adsorption isotherm for the ternary mixture of methane, nitrogen, and hydrogen on activated carbon JX101 at 313 K with bulk mole fractions of 0.3648, 0.2775, and 0.3577, respectively. Closed symbols, experimental data (WU et al., 2005). Continuous lines, proposed model.	58

List of Tables

Table 1	– Values of SAFT-VR Mie parameters for fluid-fluid interactions.	48
Table 2	– Values of wall-fluid interaction parameters (λ_{wf} and ε_{wf}) for the extended SAFT-VR Mie for confined fluids for pure methane, ethane, ethylene, and propane adsorbed on MSC5A at 303.15 K.	49
Table 3	– Average Absolute Relative Deviation (AARD) values between the adsorption isotherms predicted by the proposed model and the experimental data obtained by Konno et al. (1985).	52
Table 4	– Values of wall-fluid interaction parameters (λ_{wf} and ε_{wf}) for the extended SAFT-VR Mie for confined fluids for pure methane and nitrogen adsorbed on MOF-5 at 297 K.	52
Table 5	– Average Absolute Relative Deviation (AARD) values between the adsorption isotherms predicted by the proposed model and the experimental data obtained by Kloutse et al. (2018)	53
Table 6	– Values of wall-fluid interaction parameters (λ_{wf} and ε_{wf}) for the extended SAFT-VR Mie for confined fluids for pure methane, nitrogen, and hydrogen adsorbed on JX101 at 298 K and 313 K.	56
Table 7	– Average Absolute Relative Deviation (AARD) values between the adsorption isotherms predicted by the proposed model and the experimental data obtained by Wu et al. (2005).	56

Nomenclature

Symbols

$\langle E \rangle^{\text{CONF}}$ Energy due to confinement effect

$\langle E \rangle^{\text{IG}}$ Ideal gas energy

$\langle E \rangle^{\text{R}}$ Residual energy

A Helmholtz Free Energy

A^{ASSOC} Helmholtz free energy due to association

A^{CHAIN} Helmholtz free energy due to the formation of chains

A^{CONF} Helmholtz free energy due to confinement effects

A^{DISP} Helmholtz free energy due to dispersion forces

A^{HS} Helmholtz free energy of a system

A^{IDEAL} Ideal-gas term contribution

A^{MONO} Helmholtz free energy due to monomer contribution

A_0 Helmholtz Free Energy of the reference system

A_1 Perturbation Free Energy

C Bulk concentration at equilibrium

C_e Equilibrium concentration of the adsorbate

C_{ij} Cofactor matrix

$g(r)$ Radial distribution function

h Planck's constant

$J(n_{ads})$ Jacobian function

k Boltzmann constant

K_f	Freundlich constant
K_L	Adsorbate - adsorbent interaction constant
M	Number of association sites on each molecule
m	Number of segments
N	Number of chains
n	Amount of the component
N_s	Number of spherical segments
p_j	Momentum of each particle
q	Set of coordinates of each particle
Q	Partition function
q	Adsorbed amount
q_{max}	Limiting monolayer adsorption capacity
r	Distance from particles
T	Temperature
u	Dispersion energy parameter per segment
$U_N^{(0)}$	Potential energy of a reference system
$U_N^{(1)}$	Perturbation
U_N	Total potential energy
V	Volume
V_{ads}	Volume of the adsorbed phase
V_{bulk}	Volume of the bulk phase
x	Relative vapor pressure
X^A	Mole fraction of molecules not bonded at site A

x_s Mole fraction of segments

Z_N Configurational integral

Greek Letters

η Reduced density for pure fluids

β Reduced temperature

Γ Adsorbed amount

Λ de Broglie thermal wavelength

λ Range of attractive forces

μ Chemical potential

ν_p Specific pore volume

ρ_{ads} The adsorbed mixture density

σ Particle diameter

ε Depth of the square well potential

$\zeta_{3,i,j}$ Mixture packing fraction

ζ_l Reduced density

Contents

1	INTRODUCTION	16
2	LITERATURE REVIEW	18
3	THEORETICAL FOUNDATIONS	23
3.1	Adsorption	23
3.2	Perturbation Theory	27
3.3	Statistical Associating Fluid Theory - SAFT	29
3.4	Monte Carlo Simulation	32
4	METHODOLOGY	35
4.1	Theoretical Development	35
4.2	Computational Details	40
4.2.1	Monte Carlo Simulation	40
4.2.2	Phase equilibrium calculations	44
4.2.3	Pure component fluid-wall interaction parameters	47
5	RESULTS	48
5.1	Binary mixtures	48
5.1.1	Ternary Mixtures	53
6	CONCLUSIONS	59
	BIBLIOGRAPHY	60

1 Introduction

The thermodynamic behavior of confined fluids on a microscopic scale differs significantly from bulk fluids. This fact is associated with the intermolecular interactions between the fluid and the pore wall, and dimension and shape of the system where the fluid is inserted. As the pore dimension decreases, the effect of confinement on thermodynamic properties increases. Many chemical processes involve fluids confined in nanoporous media, for example: adsorption separations, oil and gas extraction, development of nanomaterials, design of microporous materials for methane storage (ARAGUAREN et al., 2012) (CRACKNELL; CHIMOWITZ, 1993), and chemical separations using inorganic membranes (ARAGUAREN et al., 2012) (AFRANE; GORDON; GUBBINS, 1996). In view of that, the establishment of consistent theoretical foundations of thermodynamics of confined fluids is certainly essential to advances in nanoscale technologies (KIM et al., 2011).

An appropriate description of confined fluids requires a good representation of the structure of both the pore and the fluid. Therefore, the need of an adequate representation of the various structures of the solids employed as adsorbents emerges. To simplify this problem, most of the related work uses idealized geometries to represent the pore. With regard to the fluid, a precise representation of the force field that includes both fluid-fluid interactions and fluid-wall interactions is necessary (TRAVALLONI, 2012). A versatile force field comprises the main aspects of the interactions for a broad range of real substances and is essential for determining the thermophysical properties of fluids (DUFAL et al., 2015).

The competition between the two types of interatomic forces coexisting in the system, (fluid-fluid interaction and fluid-wall interaction) is responsible for the density variation in the pore. This inhomogeneity in confined fluids is manifested in structural properties and system dynamics triggering a shift in the thermodynamic equilibrium properties and a modification of the transport properties (ZHANG; TODD; TRAVIS, 2004).

Among the various effects caused by confinement, phase behavior is one of the most studied, since this phenomenon is present in many industrial and geophysical operations. In nanoporous media, phase behavior becomes a function of both fluid-fluid interactions and fluid-wall interactions (BARSOTTI et al., 2016). The introduction of the force field due to the solid matrix results in new types of phase transitions not found in the bulk phase, and modifications in phase

transition regions (GELB et al., 1999). A better understanding of confined fluid phase equilibria is crucial to significant improvements in chemical processes. A contemporary example is the need to estimate hydrocarbon recovery in shale gas and shale oil reservoirs, which are often confined in nanometric spaces. Due to the large range of pore size distribution in this type of reservoir, the fluid behavior in shale is considerably modified. This characteristic of the reservoir directly affects the methods of reservoir evaluation and estimations of original hydrocarbons in place (BARSOTTI et al., 2016). Also in practical applications such as adsorption, the representation of the adsorbent structural heterogeneity is still a complex challenge that needs to be overcome. Traditional models used to calculate adsorption isotherms neglect the influence of shape and dimensions of the adsorbent on the adsorbed phase properties (TRAVALLONI, 2012). This deficiency in adsorption models might impact adsorption calculations in processes that use adsorbents with a broad range of pore size distribution. Therefore, it is even more evident the need for proper models that rigorously take into account the main effects of confinement.

The main objective of this project is to extend the Statistical Associating Fluid Theory (SAFT-VR Mie) equation of state for the calculation of mixture adsorption isotherms. The theoretical framework on which this model is based is the methodology formulated by Franco, Economou, and Castier (2017) for pure confined fluids. By using the generalized van der Waals theory, a term regarding the Helmholtz free energy contribution due to the confinement effect will be coupled with the SAFT-VR Mie equation of state. Once the theoretical expression for Helmholtz free energy due to confinement effect is developed, one should have a complete model which may provide a consistent description of confined fluid mixtures. Solving the phase equilibrium criteria, multicomponent isotherms are calculated applying the proposed model.

An outline of the information introduced in each chapter is presented as follow: Chapter 2 presents an overview of literature that provided important theoretical foundations for the development of equations of state for confined fluids. Chapter 3 introduces concepts that were essential to the development of our equation of state. Chapter 4 presents the methodology for the model formulation, which includes: adopted hypotheses and simplifications, model derivation, and molecular simulation specifications. In Chapter 5, the proposed model is applied to the prediction of different multicomponent adsorption isotherms. The results, advantages, and drawbacks of the model are also discussed. Finally, Chapter 6 presents the conclusions and suggestions for future works.

2 Literature Review

There is a wide variety of methods and tools available to evaluate the behavior of confined fluids. For cases in which information about the behavior at microscopic levels is necessary, techniques such as molecular simulation and density functional theory (DFT) are the most appropriate. Experimental characterization at the atomic level is also a promising path, but, due to the difficulties and lot of effort required, molecular simulation is used to help correlate experimental results with theory (JAYANT; SANG, 2007).

Prediction of the adsorption isotherms relies on the complex relationship between fluid and solid properties (BUTZ; ZIMMERMANN; ENDERS, 1998). The materials usually used as adsorbents in adsorption separation process frequently presents a complicated structure, having a large range of pore size and shape distribution, blocked and active pores, and networked pores, thus, the interpretation of adsorption in such materials is somehow quite inaccurate (BALBUENA; GUBBINS, 1993). Another difficulty regarding adsorption studies is the prediction of multicomponent isotherms. Experimental measurements of the adsorption equilibrium data of mixtures are extremely time-consuming, however, multicomponent adsorption data are crucial for the design of adsorption processes (WU et al., 2005).

Density functional theory (DFT), a method derived within statistical mechanics, has been largely applied to analyze isotherms data. In DFT, adsorption is described as a function of the pore dimension, attraction between wall and fluid molecules, and the probability of distribution of molecules in the pores of the material (BALBUENA; GUBBINS, 1993). In this technique, numerical methods are used to solve a system of nonlinear equations, and density profiles inside the pore are found. From these profiles, the calculation of thermodynamic properties is possible. This method, although less cumbersome, is less detailed than molecular simulation (TRAVALLONI, 2012).

Despite the great applicability of techniques such as DFT and molecular simulation, their use requires a great computational effort, and sometimes evaluating a fluid at microscopic level is unnecessary. In process such as adsorption, knowing the global properties of a fluid might be sufficient. From an engineering perspective, the use of analytical equations of state might be a satisfactory alternative to model confined fluids systems. Simplifications such as an average of the density variation in the porous media are considered.

Travalloni et al. (2010) extended the van der Waals equation of state to describe pure fluids and mixtures confined in porous media. The study was based on the generalized van der Waals theory. The pore geometry was assumed to be cylindrical and molecular interactions were described by a square-well potential. The approach used to extend van der Waals equation of state to describe confined fluids was set through the redefinition of expressions for the free volume and configurational energy from the canonical partition function. In the new expressions, terms associated with the main effects of the confinements on the fluids were included, such as pore radius and fluid-wall interaction parameters. This modification resulted in a more flexible model that can be simultaneously used for confined and bulk fluids.

The developed model requires only two adjustable parameters for each component of the system, concerning the interactions with the wall. These parameters were obtained by correlating pure fluids adsorption experimental data. The interaction parameters and the radius of the pore were varied to analyze the sensitivity of each variable, and different isotherms can be obtained by varying fluid-wall interaction parameters. The proposed model was used to predict calculations of several adsorption isotherms for both mixtures and pure fluids. Results showed that good correlations were obtained for pure fluids, and satisfactory predictions for mixtures (TRAVALLONI et al., 2010).

Barbosa et al. (2018) proposed a modification to Travalloni et al. (TRAVALLONI et al., 2010) work regarding the drawbacks of the model. Despite the good results, the previous approach presented an inconsistency with the ideal solution limit. This means that, for a system of two identical components and a system of pure component at the same conditions of pressure and temperature, different values of molar volume would be obtained. Travalloni, Castier, and Tavares (2014) also extended Peng-Robinson equation to describe confined fluids, and the same inconsistency is noted in the model. To develop a new model more appropriate for mixtures, Barbosa et al. (2018) based their work on the previous approach, using similar steps to extend equations of state to describe confined fluids. To correct the inconsistency, explicit mixing rules were introduced in the model. Furthermore, the equation was adapted for spherical pores. As expected, the new model presented better results when describing mixtures than the previous one; also, this study was extremely important to understand how different pore geometries impact the model performance.

A different approach to extend van der Waals equation of state is proposed by Zarragoicochea and Kuz (2002). The authors showed that, for a fluid restricted in pores of microscopical dimensions, phase equilibrium is dependent on the system size. Considering a pore of infinite

length, the confined fluid pressure has a tensorial aspect. Thus, a new model for Helmholtz free energy is calculated, and from this expression, the axial and transversal components of the pressure tensor are obtained. From the axial fluid pressure the critical parameters are given. In this model, particles are considered to interact via Lennard-Jones potential. This work is extremely relevant to predict capillary transitions and also to show that confinement can lead to a shift of the critical parameters compared to the bulk fluid. The results presented good correlation with experimental data, even though the interaction between fluid and wall was neglected.

Afterwards, Zarragoicoechea and Kuz (2004) used the same model to evaluate the shift on the critical temperature as a function of the pore size. The model proved to be consistent since a good agreement between the theory and experiment was observed, also no parameter fitting was needed in the model. In addition, the equation was able to predict a shift in the critical pressure, although this fact was not confronted with experiments.

Among the traditional approaches, cubic EoS's have been used extensively. This class of models is inadequate to describe self associating fluids despite its considerable popularity (GIL-VILLEGAS et al., 1997). This limitation imposes the need for new models that describe the phase behavior of more complex fluids. Many principles of statistical mechanics were applied toward significant developments of equations of state such as SAFT (Statistical Associating Fluid Theory), a semi empirical EoS that was adjusted for several range of fluids, including organic compounds, light gases, water, and polymers (ECONOMOU, 2002). Since then, some studies of adsorption isotherms were formulated using this equation.

Franco, Economou, and Castier (2017) extended the SAFT-VR Mie equation of state to calculate adsorption isotherms of a pure fluid. In this work, a theoretical model to describe the structure consequent from the fluid-solid interaction was developed and then compared with Travalloni et al.(2010) empirical expression. The interactions between molecules were described by a square-well potential, and the effect of confinement on the association and formation of chains between molecules was neglected.

To adapt SAFT-VR Mie equation of state to describe confined fluids, a term relative to the Helmholtz free energy due to confinement was coupled with the equation of state. The theoretical development of this term derives from the calculation of the residual energy resulted from the confinement, based on the generalized van der Waals framework (FRANCO; ECONOMOU; CASTIER, 2017).

Solving a phase equilibrium problem, the formulated model was then used to calculate adsorption isotherms in two different cases: light hydrocarbons adsorbed in a carbon molecular

sieve, and carbon dioxide, nitrogen, and water adsorbed in a zeolite. For the first case, the theoretical and the empirical expression for the pore structure were compared with experimental data. The theoretical formulation presented better agreement with experimental data than the empirical one.

Martínez, Trejos, and Gill-Villegas (2017) based on Statistical Associating Fluid Theory for potentials of Variable Range framework developed the 2D-SAFT-VR approach to model the adsorption isotherms for binary mixtures. This approach was mathematically formulated considering that the particle-particle and particle-wall interactions are modeled by square-well potentials. Assuming that the substrate modifies the pair potential energy of the adsorbed molecules, the square-well parameters are considered to be different for the bulk and adsorbed segment-segment. The 2D-SAFT-VR model was used to predict adsorption of water and methanol onto activated carbons, metal organic frameworks and carbon molecular sieve membranes. The association part was derived for molecules with two, three, and four association sites. The model results were compared to experimental data presenting quite good performance.

The Random Surface (RS)-SAFT is a new version of the SAFT-DFT developed by Aslyamov, Pletneva and Khlyupin (2019). Considering that most of the natural materials used as adsorbent are geometrically heterogeneous, and that nano-roughness has a great impact in adsorption, this novel model major advantage is the prediction of adsorption considering rough surfaces. The SAFT-VR Mie EoS is used as the base for the homogeneous bulk limit, however a modification in the intermolecular term of Helmholtz free energy was made to extend the equation to inhomogeneous fluids. To account for a real surface, RSDFT method was employed. In Aslyamov, Pletneva, and Khlyupin (2019) previous work, a model was developed to predict the surface geometry based on experimental isotherms. The developed approach was used to analyze hexane adsorption on carbon black. Experimental data were used to tune RSDT and to obtain the adsorbent surface. Given obtained features of the pore, RS-SAFT was used to calculate adsorption isotherms.

Equations of state have been one of the most promising ways of describing confined fluids, since analytical expressions are practical and simple for industrial applications. Cubic equations of state are not always the best option as they present a great limitation for uncovering some types of fluids such as self-associating and highly dense fluids. In view of that, SAFT equations of state show great advantage as they make possible to describe the properties of a greater range of complex fluids. Considerable work has been done in developing consistent models for inhomogeneous systems, and certainly, these studies improved our understanding of confined

fluids properties. However there are still gaps in the literature regarding models that take into account, in comprehensive and non-generalist way, the structural characteristics of adsorbent solids.

3 Theoretical Foundations

3.1 Adsorption

Adsorption is a separation process characterized by transferring a particular component of a fluid phase to the surface of a solid (adsorbent). The adsorption can be classified according to the intensity of forces involved in the process. When the interaction between the adsorbate and the surface of the adsorbent is weak, the adsorption is classified as physisorption. In this case, the forces involved are mainly van der Waals forces. In chemisorption, the electronic structure of the molecules are modified, leading to the formation of chemical bonds with the substrate (NASCIMENTO et al., 2014).

A lot of factors is known to influence in the adsorption phenomenon, for example: the adsorbent and adsorbate characteristics, and the process operating conditions. Some of the fluid molecules are more likely to attract to the surface because of their molecular weight, shape, and polarity. The surface area and pore size of the adsorbent are also very relevant. If pores are too small, larger molecules are hindered from being held on the pore (MCCABE; SMITH; HARRIOT, 1993). The operating conditions also play an important role. The temperature directly affects the adsorption rate constant, and the pH of an adsorption process in solution controls the adsorbent surface charge (NASCIMENTO et al., 2014; TOLEDO et al., 2005).

The adsorption isotherms are defined by the equilibrium relationship between the concentration in the fluid phase, and the concentration in the adsorbent particles (MCCABE; SMITH; HARRIOT, 1993). The adsorption isotherms are classified in six main types as shown in Figure 1 .

- Type I:

This isotherm is described by the classical Langmuir's equation. In this isotherm, even at high pressures of the gas phase, the adsorbed amount tends asymptotically to a constant value. This limiting value represents the completion of a surface monolayer (KELLER; STAUDT, 2005).

- Type II:

This isotherm is generally described by the Brunauer–Emmett–Teller (BET) model. At

low pressures it shows a surface monolayer. Point "B" in the curve, represents the completion of an adsorbed monolayer. At high pressures, the isotherm shows multilayer adsorption (KELLER; STAUDT, 2005; CHIOU, 2002).

- Type III:

The main feature of this type of isotherm is the weak interaction between the fluid phase and the surface compared to the fluid-fluid interaction (KELLER; STAUDT, 2005; CHIOU, 2002).

- Type IV:

This type of isotherm is characteristic of mesoporous materials. This isotherm presents pore condensation with hysteresis behavior (KELLER; STAUDT, 2005; CHIOU, 2002).

- Type V:

This is very rare type of isotherm. Similar to type IV, there is capillary condensation and hysteresis. In this isotherm, the forces between adsorbent and adsorbate are weaker compared to adsorbate-adsorbate interactions. (KELLER; STAUDT, 2005; ROMANIELO, 1999).

- Type VI:

This isotherm shows multilayer adsorbates which become more pronounced at low temperatures (KELLER; STAUDT, 2005).

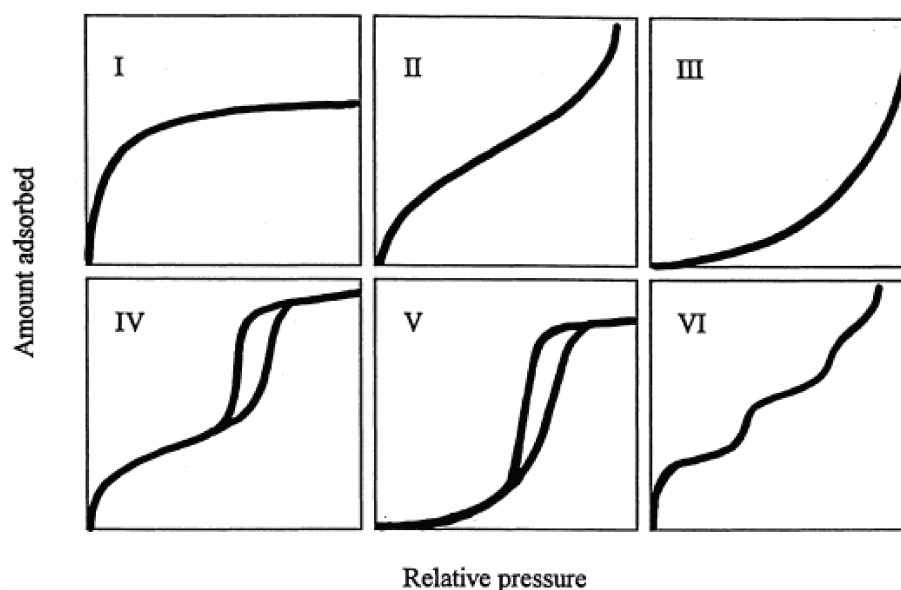


Figure 1 – The six types of isotherm (IUPAC classification) (KELLER; STAUDT, 2005)

The adsorption phenomenon has been widely applied for different industrial purposes. For example, the separation and purification of liquid and gas mixtures, drying gases and liquids before loading them into industrial systems, removal of impurities from liquid and gases, recovery of chemical from industrial gases and water treatment (DRABOWISKI, 2001). In such processes, the information about the amount adsorbed in the porous materials at a given pressure and temperature is provided by the calculation of adsorption isotherms. Generally, three major paths are used to derive mathematical equations for adsorption isotherms. The first consists of using kinetic expressions for adsorption and desorption rates in equilibrium. The second is based on classical thermodynamics making an analogy with the ideal solution theory. The third path is based on statistical thermodynamics.

Among the existing kinetic models to predict adsorption, the most commonly used are Langmuir, Freundlich, and BET isotherm models.

- Langmuir adsorption isotherm: In Langmuir's model, the adsorption is assumed to occur in a fixed number of sites, and each site can only take one molecule. Also, these sites are considered to be energetically equivalent and no interaction exists between adsorbed molecules (KELLER; STAUDT, 2005).

$$q = \frac{q_{max}K_L C_e}{1 + K_L C_e} \quad (3.1)$$

In Equation 3.1, q is the adsorbed amount and q_{max} is the limiting monolayer adsorption capacity. In other words, q_{max} represents the formation of monolayer when the adsorbed vapor covers completely the surface of the sorbent. C_e is the equilibrium concentration of the adsorbate, and K_L is the adsorbate - adsorbent interaction constant.

- Freundlich equation: unlike the Langmuir isotherms, the Freundlich model is an empirical equation which is not theoretically based. This equation was developed to account for adsorption on heterogeneous solid surfaces (DRABOWISKI, 2001). The general form of this equation is:

$$q = K_f C^n \quad (3.2)$$

where q is the amount adsorbed, C is the bulk concentration at equilibrium, K_f is the Freundlich constant, and n is an exponent related to the solute adsorption.

- BET multilayer adsorption theory: the Brunauer–Emmett–Teller (BET) theory, which is somehow a generalization of Langmuir isotherm, was developed to predict multilayer adsorption on solids (DRABOWISKI, 2001). This model is based on the following assumptions: Langmuir’s equation applies to each adsorption layer, adsorption and desorption take place only in the layer that is exposed, and the heat of adsorption in the first layer is always higher than the subsequent ones (CHIOU, 2002).

$$\frac{q}{q_m} = \frac{C_x}{(1-x)[1+(C-1)x]} \quad (3.3)$$

where q and q_m are the amount adsorbed and the monolayer capacity respectively, x is the relative vapor pressure, and C is a constant related to the difference between the heat of adsorption in the first layer and the heat of liquefaction of the vapor (CHIOU, 2002).

Models such as Langmuir and Freundlich are extensively used to calculate adsorption, because they can describe well experimental data, and require only two parameters (NASCI-MENTO et al., 2014).

Regarding the numerous adsorption models based on classical thermodynamics, one of the most successful is the *IASM* model (Ideal Adsorbed Solution Model) developed by Myers and Prausnitz (1965). In this model, the adsorbed phase is assumed to be ideal. The key feature of this method is an analogy with Raoult’s law for vapor-liquid equilibrium. *IASM* is referenced as a remarkable model for the prediction of mixture adsorption equilibrium using only pure-component adsorption isotherms. Nevertheless, the model presents some drawbacks: for mixtures in which one component present significant difference in size and polarity compared to others, or, if the adsorbent has a heterogeneous surface, the model does not show good performance (WALTON; SHOLL, 2015).

The statistical thermodynamics enables the formulation of a molecular theoretical model to predict the properties of a macroscopic system. Based on this framework, the system is considered to be composed of a large number of molecules, therefore, the main purpose is to obtain the thermodynamic properties using information about the molecular properties and interactions. An example of statistical theory applied to adsorption is the statistical model adsorption isotherm (SSTM) developed by Ruthven and coworkers, a method that is usually applied to predict adsorption in zeolites (ROMANIELO, 1999).

3.2 Perturbation Theory

A significant step was recently taken motivated by the necessity of equations of state that represent fluids that could not be described by the traditional models. The path towards these models has been traced through the development of Wertheim's Thermodynamic Perturbation Theory (TPT) within statistical mechanics. A seminal argument for this important theory lies in the fact that the structure of the liquid is mainly determined by the short range repulsive forces, and the attractive forces of the potential are dedicated to keep the molecules together at a fixed density (MCQUARRIE, 2000). From this argument, the idea to treat a fluid as a system of repulsive interactions and depict attraction forces as a perturbation, emerges.

In Perturbation Theory, a reference system, in which only repulsive interactions exist, is chosen. The potential frequently used to describe this reference system is the hard-sphere potential. In view of that, any deviation of a real system that might cause variations in the thermodynamic behavior of the reference system is considered a perturbation. Thus, this perturbation can assume the form of different factors, such as van der Waals attractive interactions, association interaction, and the non-spherical shape of the molecules (KLEINER; TUMAKAKA; SADOWSKI, 2009). The total potential energy of a system can be written as a sum of the potential energy of a reference system (unperturbed), which is usually a hard-sphere system $U_N^{(0)}$, and the perturbation $U_N^{(1)}$.

$$U_N = U_N^{(0)} + U_N^{(1)} \quad (3.4)$$

The configurational integral of the total potential is:

$$Z_N = \int \cdots \int \exp(-\beta[U_N^{(0)} + U_N^{(1)}]) d\mathbf{r}_1 \cdots d\mathbf{r}_N \quad (3.5)$$

Where $\beta = 1/k_B T$.

Multiplying and dividing the configurational integral by :

$$\int \cdots \int \exp(-\beta U_N^{(0)}) d\mathbf{r}_1 \cdots d\mathbf{r}_N \quad (3.6)$$

The configurational integral can be rewritten as:

$$Z_N = Z_N^{(0)} \langle \exp(-\beta U_N^{(1)}) \rangle_0 \quad (3.7)$$

This strategy enables us to write the configurational integral as a weighted average of $\exp(-\beta U_N^{(1)})$ over the unperturbed system.

The Helmholtz free energy is an important property in thermodynamics. With it, all other thermodynamic properties can be obtained. From Equation 3.7, it is possible to write the

Helmholtz free energy as a sum of the Helmholtz free energy of the reference system and the perturbation free energy:

$$A = A^{(0)} + A^{(1)} \quad (3.8)$$

From the canonical partition function, $Q = Z_N/(N!\Lambda^{3N})$, the Helmholtz free energy might be calculated as:

$$A = -kT \ln Q \quad (3.9)$$

$$-\beta A = \ln \left(\frac{Z_N^{(0)}}{N!\Lambda^{3N}} \right) + \ln \langle \exp(-\beta U_N^{(1)}) \rangle_0 \quad (3.10)$$

Hence, we can infer that:

$$A^{(1)} = -kT \ln \langle \exp(-\beta U_N^{(1)}) \rangle_0 \quad (3.11)$$

The term $\exp(-\beta A^{(1)})$ is expanded in powers of β , and each coefficient of β^n is defined as w_n :

$$\exp(-\beta A^{(1)}) = \sum_{k=0}^{\infty} \frac{(-\beta)^k}{k!} \langle U_N^{(1)k} \rangle_0 \quad (3.12)$$

$$w_1 = \langle U_N^{(1)} \rangle_0 \quad (3.13)$$

$$w_2 = \langle (U_N^{(1)})^2 \rangle_0 - \langle U_N^{(1)} \rangle_0^2 \quad (3.14)$$

$$w_3 = \langle (U_N^{(1)})^3 \rangle_0 - 3\langle (U_N^{(1)})^2 \rangle_0 \langle U_N^{(1)} \rangle_0 + 2\langle (U_N^{(1)}) \rangle_0^3 \quad (3.15)$$

Therefore, the Helmholtz free energy at high temperatures can be written as follows:

$$A = A_0 + w_1 - \frac{w_2}{2kT} + O(\beta^2) \quad (3.16)$$

The term w_1 is relatively simple and can be written as:

$$w_1 = \frac{\rho^2 V}{2} \int u^{(1)}(r_{12}) g_o^{(2)}(r_{12}) dr_{12} \quad (3.17)$$

where g_o is the radial distribution function of the reference system.

Nonetheless, the second term in the expansion is more complex, since it accounts for the distribution function of three and four body, which is not easily calculated. Barker and Henderson (1967) developed a method to approximate w_2 . In their approach, considering an unperturbed

system, the range of intermolecular distances is divided in intervals $r_j - r_{j+1}$, at each interval, the probability to find N_j molecules is $P(N_j)$. The perturbing potential is considered constant assuming that the intervals are small. Based on these assumptions, an expression called local compressibility approximation is derived to calculate w_2 (MCQUARRIE, 2000):

$$A\beta = A^0\beta + \frac{\rho\beta}{2} \int u^{(1)}(r)g_o(r)4\pi r^2 dr - \frac{\rho\beta^2}{4} \int [u^{(1)}(r_{12})]^2 kT \left[\frac{\partial \rho g_o}{\partial p} \right] 4\pi r^2 dr + O(\beta^3) \quad (3.18)$$

The Perturbation Theory was the basis for the development of the statistical associating fluid theory (SAFT). The SAFT equations of state are emerging as an accurate and versatile family of models due to the wide range of fluids to which they are applied. As previously stated, these models respond to the need of describing fluids with highly directional attractive forces, for example, fluids with hydrogen bonds (GIL-VILLEGAS et al., 1997).

3.3 Statistical Associating Fluid Theory - SAFT

Equations of State (EoS) were settled as a fundamental tool in simulation and optimization of several processes in industry. They fulfill the necessity of describing volumetric behavior, vapor-liquid equilibria, and the thermal properties of fluids in different pressure, temperature, and compositions with low computational cost. van der Waals was the first to introduce an equation of state, since then numerous EoS were proposed. In general, we can divide the equations of state in two categories, cubic and non cubic. The cubic EoS's are widely used in industry due to the simplicity of its mathematical formulation. Among the EoS of this group, the most popular are Soave-Redlich-Kwong (SRK) (1972) and Peng-Robinson (PR) (1976) (ASHOUR et al., 2011). In the category of non cubic EoS, the Statistical Associating Fluid Theory (SAFT) emerged as a successful model. SAFT is a molecular based EoS that considers a molecule as a chain of tangential spherical segments (CHAPMAN et al., 1989). This EoS has drawn special attention due to the great range of types of fluids that it is able to accurately describe, such as associating fluids, copolymers and electrolytes, which are fluids that cannot be described by traditional cubic EoS (ECONOMOU, 2002). SAFT equation of state was first developed by Chapman et al. (1989) based on the thermodynamic perturbation theory of Wertheim. This equation of state is written as a sum of terms that represent different intermolecular forces to the Helmholtz free energy. Once the Helmholtz free energy of the fluid is known, standard thermodynamic equations can be used to calculate important thermodynamic properties such as pressure and chemical potential (ECONOMOU, 2002). A great advantage of a molecular based equation of

state is the possibility of distinguishing the effects of molecular structure on bulk properties and phase behavior. The Wertheim's perturbation theory was the theoretical basis used to account for the effects on Helmholtz free energy of association and chain formation. In a very simplified way, the main point of this theory is the connection between association strength and monomer density. A brief explanation of the mathematical expression of each intermolecular contribution is given based on the original version of SAFT developed by (CHAPMAN et al., 1989). A SAFT EoS can generally be written as:

$$A = A^{\text{IDEAL}} + A^{\text{MONO}} + A^{\text{CHAIN}} + A^{\text{ASSOC}} \quad (3.19)$$

- Ideal Contribution

The ideal-gas term contribution is given by:

$$\frac{A^{\text{IDEAL}}}{RT} = \ln(\rho\Lambda^3) - 1 \quad (3.20)$$

In this expression, ρ is the number density of chain molecules and Λ^3 represents the de Broglie volume.

- Monomer contribution

This contribution represents the segment-segment interactions. Examples of this type of interaction are hard-sphere and dispersion forces. Thus we can write that:

$$\frac{A^{\text{MONO}}}{RT} = \frac{A^{\text{HS}}}{RT} + \frac{A^{\text{DISP}}}{RT} \quad (3.21)$$

The term A^{HS} represents the Helmholtz free energy of a hard-sphere reference system. This term is calculated using the Carnahan-Starling expression (CARNAHAN; STARLING, 1969):

$$\frac{A^{\text{HS}}}{RT} = m \frac{4\eta - 3\eta^2}{(1 - \eta)^2} \quad (3.22)$$

where m is the number of segments per molecule, and η the packing fraction.

The dispersion force is the weakest intermolecular force that is present between molecules when they are relatively close. The Helmholtz free energy due to the dispersion forces effects is calculated as follows:

$$\frac{A^{\text{DISP}}}{RT} = m \frac{u}{kT} \left(a_1^{\text{DISP}} + \frac{u}{kT} a_2^{\text{DISP}} \right) \quad (3.23)$$

- Chain contribution

The contribution to the Helmholtz free energy due to the formation of chains of m monomers is given by:

$$\frac{A^{\text{CHAIN}}}{RT} = \sum_i X_i (1 - m_i) \ln(g_{ii}(d_{ii})^{\text{HS}}) \quad (3.24)$$

In this expression, g_{ii} is the hard sphere correlation function for a pair of molecules evaluated at the contact.

- Association contribution

This term accounts for site-site specific interactions of the segments, one example of this contribution are the hydrogen bond interaction. The Helmholtz free energy due to association is determined from the expression:

$$\frac{A^{\text{ASSOC}}}{RT} = \sum_{A=1}^M \left[\ln X^A - \frac{X^A}{2} \right] + 0.5M \quad (3.25)$$

where M is the number of association sites on each molecule and X^A is the mole fraction of molecules not bonded at site A.

The SAFT equation of state is continually being modified to improve its accuracy. Nowadays there are numerous versions of this equation. Some of the more relevant versions will be outlined here.

The SAFT-VR equation of state was developed by Gil-Villegas and co-workers (1997). In this version, hard-core monomers are considered to interact with an arbitrary potential of variable range, namely square-well, Sutherland, and Yukawa. The monomer Helmholtz free energy is expressed as a series of expansion of the inverse of temperature. The first two perturbation terms were taken into account, and the Barker and Henderson perturbation theory was used to approximate these functions. The monomer background correlation function is also derived to account for structure of the new reference fluid, therefore the chain and association terms of the equation were consequently modified.

Gross and Sadowski (2001) proposed another important contribution to the family of SAFT equations of state: the Perturbed-Chain SAFT (PC-SAFT). Instead of applying a perturbation theory of second order to the reference system of hard-spheres as previous works, the perturbation theory is applied to a hard-chain system. The main idea of this model is to account for the influence of the non-spherical shape of the molecule in the dispersion term. The contributions regarding association and chain formation remain calculated as in the original equation.

Laffite and co-workers (2013) proposed the approach we chose to use in this work, the SAFT-VR Mie equation of state. This new version of SAFT uses the Barker and Henderson high-temperature perturbation expansion up to the third order in the free energy of the monomer Mie system. Also, the radial distribution function of the reference monomer fluid is calculated from a second-order expansion. All these improvements make the SAFT-VR Mie equation a useful tool that can be applied to a broad range of interactions.

3.4 Monte Carlo Simulation

A further study of a fluid physical properties requires a good representation of the intermolecular potential energy between molecules, and the solution of the equations of statistical mechanical for the system considering a given potential (GELB et al., 1999). With regard to the statistical mechanical equations, molecular simulation techniques represent a precise approach that numerically solve these equations using a computer. Successful examples of these techniques are: Molecular Dynamics and Monte Carlo simulations. These methods allow a modeling of the system at a molecular level providing important information about the structure and thermodynamic properties of a fluid. However, their main limitation resides on the appropriate description of the used force field, and the large computational effort needed (BARLETTE; FREITAS, 1999).

The partition function establishes a connection between the mechanical energy states of a microscopic system and the thermodynamic properties of that system (MCQUARRIE, 2000). Considering a system with a large number of particles, the total energy is given by the Hamiltonian function $H(\mathbf{p}, \mathbf{q})$. Therefore we can assume that:

$$Q = \sum_j \exp(-\beta\varepsilon) = \frac{1}{N!h^{sN}} \int \cdots \int \exp(-\beta H(\mathbf{p}, \mathbf{q})) d\mathbf{p} d\mathbf{q} \quad (3.26)$$

$$H(\mathbf{p}, \mathbf{q}) = \frac{1}{2m} \sum_{j=1}^N (p_{xj}^2 + p_{yj}^2 + p_{zj}^2) + U(\mathbf{q}_1, \cdots, \mathbf{q}_N) \quad (3.27)$$

In the Hamiltonian function, p denotes a set of p_j that is the momentum of each particle, and q the set of generalized coordinates for each particle.

The momenta integration can be solved analytically, however the part of the integral that contains the intermolecular forces are mathematically complicated to solve due to the dependence on the relative distance between molecules. This part of the integral is named the configuration

integral (Z):

$$Q = \frac{1}{N!} \left(\frac{2\pi mkT}{h^2} \right)^{3N/2} Z_N \quad (3.28)$$

where

$$Z = \int_V \exp(-U(\mathbf{q}_1, \dots, \mathbf{q}_N)/kT) d\mathbf{q}_1 \dots \mathbf{q}_N \quad (3.29)$$

The calculation of the average value of some property $\langle A \rangle$ is given by the following equation:

$$\langle A \rangle = \frac{\int d\mathbf{q}^N \exp[-\beta U(\mathbf{q}^N)] A(\mathbf{q}^N)}{\int d\mathbf{q}^N \exp[-\beta U(\mathbf{q}^N)]} \quad (3.30)$$

where \mathbf{q}^N is the position of all N particles. The probability of finding the system in a determined configuration is calculated as follows:

$$\rho(\mathbf{q}^N) = \frac{\exp[-\beta U(\mathbf{q}^N)]}{\int d\mathbf{q}^N \exp[-\beta U(\mathbf{q}^N)]} \quad (3.31)$$

If we consider that it is possible to randomly generate N_{MC} points in configuration space, Equation 3.30 can be rewritten as :

$$\langle A \rangle = \frac{1}{N_{MC}} \sum_{i=1}^{N_{MC}} A_i(\mathbf{q}^N) \quad (3.32)$$

Monte Carlo simulation is a technique that enables the calculation of an average property by approximating the configuration integral in Equation 3.30 of a sum of random points in space. The importance sampling is a method that permits to choose random numbers from a distribution in a region of the space that will make more contributions to the integral (EARL; DEEM, 2008) (BARLETTE; FREITAS, 1999). The generation of a sequence of random states is quite difficult since, by the end of the simulation, each state must have occurred with an adequate probability. Therefore, the main target is to find a method to properly generate these random numbers. To overcome this problem, the Markov chain of states method is employed (ALLEN; TILDESLEY, 2017).

Markov chains are one of the most important stochastic process. The key feature of this method is that the probability of the next state of the system is only dependent on the present state. For the development of a Markov chain, a transition matrix has to be defined (ALLEN; TILDESLEY, 2017). The transition matrix, π_{mn} , provides information about the probability of the system moving to another state or not. Therefore, if a system is in a state m , the probability to move to state n is given by π_{mn} . Let us assume that ρ is a vector that contains the probability of

a system being in a determined state, the probability vector for subsequent points will be given by:

$$\rho^j = \pi \rho^{j-1} \quad (3.33)$$

Applying the transition matrix numerous times, the chain converges to a stationary distribution, thus we can write that:

$$\rho^* = \lim_{N_{MC} \rightarrow +\infty} \rho^{(0)} \pi^{MC} \quad (3.34)$$

where ρ^* is the limiting distribution and $\rho^{(0)}$ is the probability vector for a initial configuration. Implementing the Markov chain method to our problem, the limiting distribution is the vector $\rho_m = \rho_{NVT}(\mathbf{q}_m^N)$ for each point \mathbf{q}_m^N in the phase space. Despite the limiting distribution being known, the transition matrix is undefined, therefore the question of when the move will be accepted or rejected remains.

To calculate the transition matrix, the Metropolis method was employed. First, a stochastic matrix α is specified with a single constraint: $\alpha_{mn} = \alpha_{nm}$. Next, a random particle is chosen and moved in each of the coordinate directions. Considering that the system is going from state m to state n , the following analysis is required:

If the energy of state n is lower than state m , than the new configuration is accepted, thus:

$$\pi_{mn} = \alpha_{mn} \quad \rho_n \geq \rho_m \quad (3.35)$$

If the energy of state n is greater than state m , then the move is accepted with a probability $\frac{\rho_n}{\rho_m}$:

$$\pi_{mn} = \alpha_{mn} \frac{\rho_n}{\rho_m} \quad \rho_n < \rho_m \quad (3.36)$$

hence,

$$\frac{\rho_n}{\rho_m} = \exp(-\beta[U(n) - U(m)]) \quad (3.37)$$

To accept this movement with this probability, a random number is chosen from an interval, $[0, 1]$ and compared with the probability $\frac{\rho_n}{\rho_m}$. If this number is less than $\frac{\rho_n}{\rho_m}$, the new configuration will be accepted. If the movement is rejected, the system will stay in the old configuration m . Therefore the transition matrix is calculated by:

$$\pi_{mn} = 1 - \sum_{n \neq m} \pi_{mn} \quad (3.38)$$

4 Methodology

4.1 Theoretical Development

The understanding of the thermodynamic behavior of a fluid is substantially related to the types of intermolecular forces governing molecular interactions. Specially in mixtures, determining the thermodynamic properties becomes quite complicated, since the interactions between all different components of the mixture must be evaluated. In separation processes, much of the information on the prediction of phase equilibria can be understood from intermolecular forces. The bridge that operates between intermolecular forces and macroscopic forces is statistical mechanics (PRAUSNITZ; LICHTENTHALER; AZEVEDO, 1999). However, a direct application of this technique is unfeasible due to a lot of difficulties in calculation. Thermodynamic models such as equations of state are frequently used to solve chemical engineering calculations such as phase equilibria prediction. According to Sandler (1985), a theoretical thermodynamic model presents some advantages compared to the empirical ones: the model can be derived for a particular fluid, and the parameters required are reduced in number and related to molecular properties. In view of that, Sandler extended Vera and Prausnitz seminal generalized van der Waals theory (GVDW) aiming to provide a theoretical thermodynamic model based on statistical mechanics for the derivation of equations of state.

The main contribution of the present work is to develop a model that predicts the behavior of confined fluids. The approach proposed in this work is to couple with the SAFT-VR Mie equation of state the term A^{CONF} that takes into account the residual Helmholtz free energy due to the confinement effect as shown in Equation 4.1. The theoretical formulation of such term is rooted on the generalized van der Waals theory. Plugging the Helmholtz free energy to the confinement effect to SAFT-VR Mie EoS, the total the Helmholtz free energy becomes:

$$A = A^{\text{IDEAL}} + A^{\text{MONO}} + A^{\text{CHAIN}} + A^{\text{ASSOC}} + A^{\text{ACONF}} \quad (4.1)$$

Before exploring the details of the theoretical formulation of this model, some important assumptions on which this framework relies are listed:

- Although it is well known that some adsorbents present a structural heterogeneity, in this approach a single pore size is considered.

- The roughness of the pore surface is not taken into account.
- The molecular interaction between fluid and the confining material is represented by the square-well potential. As in Franco, Economou, and Castier (2017) work, the fluid-fluid and wall-fluid interactions are decoupled, and the molecular interaction between the confining material and the fluid close to the wall is modeled as an extra potential between fluid molecules.
- The effect of confinement on chain formation and association is considered negligible. The inclusion of such effects in the modeling would require a complete redefinition of the model, taking into account the effects of the surface both on the chain (knowing that preferential orientations are important) and on the association. Since the present model disregards these phenomena, it is somehow restricted to mixtures of small molecules, with negligible surface effect on the association.

The theoretical development of the term concerning the Helmholtz free energy due to confinement effect starts with the calculation of the residual energy using the generalized van der Waals theory. The canonical average of the residual energy is represented as follows:

$$\langle E \rangle^R = \langle E \rangle - \langle E \rangle^{\text{IG}} = - \left(\frac{\partial \ln Z(N_s, V, \beta)}{\partial \beta} \right)_{N_s, V} \quad (4.2)$$

At $\beta = 0$, only the repulsive forces between molecules are relevant. Therefore, we can assume that $Z(\beta = 0)$ is a hard-sphere configuration integral. Since this limit would require the calculation of the free volume imposing a modification in the whole equation of state, for the sake of simplicity, this limit is changed to an ideal gas. This introduces a degree of inconsistency in the model. Integrating Equation 4.2 from $\beta = 0$ to β , and isolating the configurational integral:

$$Z = V^{N_s} \exp \left(- \int_0^\beta \langle E \rangle^R d\beta \right) \quad (4.3)$$

Applying Equation 4.3 to calculate the canonical partition function we have:

$$Q(N_s, V, \beta) = \frac{V^{N_s}}{N_s! \Lambda^{3N_s}} \exp \left(- \int_0^\beta \langle E^R \rangle d\beta \right) \quad (4.4)$$

where V is the volume, N_s the number of segments, Λ the de Broglie thermal wavelength, and $\langle E \rangle^R$ the canonical average of the residual energy.

Once the canonical partition function is known, properties such as the Helmholtz free energy can be obtained:

$$A^R = \frac{1}{\beta} \int_0^\beta \langle E \rangle^R d\beta \quad (4.5)$$

The potential chosen in this work to describe the interaction between the solid wall and the fluid is the square-well potential. Even though continuous potentials are more realistic, idealistic potentials like square-well simplifies the mathematical treatment of the statistical mechanical equations. This potential can be expressed by the following equation:

$$\frac{u^{SW}(x)}{\varepsilon} = \begin{cases} +\infty, & \text{if } x \leq 1 \\ -1, & \text{if } 1 \leq x < \lambda \\ 0, & \text{if } x \geq \lambda \end{cases} \quad (4.6)$$

where x is the reduced distance defined by $x = r/\sigma$, σ is the particle diameter, ε is the depth of the square-well potential, and λ is the range of the attractive forces.

For systems in which molecular interactions between the fluid and the wall are described by square-well potential, the interior of a pore can be divided in three regions, as shown in Figure 2. In region I, there are only interactions between fluid molecules, because it is a region that is beyond the range of interactions with the wall. Region II represents both fluid-fluid interactions and fluid-wall interactions. Region III is inaccessible to the centers of mass of the fluid molecules.

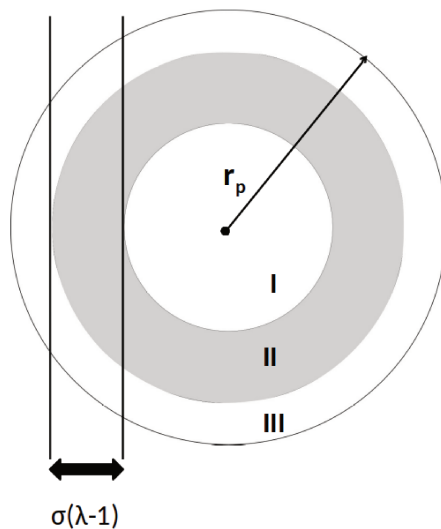


Figure 2 – Regions inside a pore for a fluid that interacts via square-well potential

To calculate the Helmholtz free energy due to the confinement effect, the residual energy due to the confinement effect has to be derived. Considering that the interaction energy between pair of molecules (pairwise additivity), an equation for residual energy due to confinement effect using a square-well potential may be described for a mixture of C components as:

$$\langle E \rangle^{\text{CONF}} = - \sum_{i=1}^C \sum_{j=1}^C \frac{N_i m_i N_j m_j \varepsilon_{ij}}{2V} \int_{\Omega} g_{ij}(x) d\Omega \quad (4.7)$$

where Ω represents the space in the pore where the fluid is attracted by the wall, V the pore volume, and N_i and m_i represents respectively the number of chains and the number of segments per chain for molecule i .

Equation 4.7 can then be rewritten as:

$$\langle E \rangle^{\text{CONF}} = - \sum_{i=1}^C \sum_{j=1}^C \frac{N_i m_i N_j m_j}{\left(\sum_{k=1}^C N_k m_k \right)} \varepsilon_{ij} \Phi_{ij} \quad (4.8)$$

where:

$$\Phi_{ij} = \frac{\left(\sum_{i=1}^C N_i m_i \right)}{2V} \int_{\Omega} g_{ij}(x) d\Omega \quad (4.9)$$

For a complete representation of the Helmholtz free energy model, an accurate expression for Φ is required. However, a precise description of Φ is associated with a complete knowledge of the confined fluid structure (FRANCO; ECONOMOU; CASTIER, 2017). To simplify the calculation of this term, the assumption regarding the decoupling of the two types of intermolecular forces is applied here. Based on that, the fluid might have two different structures: one resulting from interactions between fluid molecules and another from the fluid interaction with the confining material. Such an approach imposes that the structure of the confined fluid represented by Φ_{ij} comes from the fluid-solid interaction. The following step consists of developing a model for the calculation of Φ_{ij} .

Applying the mean value theorem to Equation 4.9, one can write:

$$\Phi_{ij} = g_{ij}(\xi_{ij}) \bar{\Phi}_0 \quad (4.10)$$

where $g_{ij}(\xi_{ij})$ is the mean value of $g_{ij}(x)$, and $\bar{\Phi}_0$ is the uniform distribution for a mixture given by the following linear mixing rule:

$$\bar{\Phi}_0 = \sum_{i=1}^C \frac{N_i m_i}{\left(\sum_{k=1}^C N_k m_k \right)} \Phi_{0,ii} \quad (4.11)$$

where $\Phi_{0,ii}$ depends on both the shape and the size of the pore:

$$\Phi_{0,ii} = 1 - \left(\frac{2r_{p,ii}/\sigma_{ii} + 1 - 2\lambda_{ii}}{2r_{p,ii}/\sigma_{ii} - 1} \right)^d \quad (4.12)$$

where $r_{p,ii}$ is the pore radius, and d is the pore dimensionality: $d = 1$ for slit pores, $d = 2$ for cylindrical pores, $d = 3$ for spherical pores, and non-integer values of d might indicate fractal pore geometries.

The expression for Φ_{ij} is where the main effects of confinement are inserted in the equation of state. Thus, Φ_0 accounts for the effect of confinement due to geometric constraints, such as shape and diameter of the pore and $g(\xi)$ the effect of confinement due to fluid-wall interaction.

For several monomer potentials, wide range of densities, and for different ranges of the potential, ξ is close to the contact value of one (GIL-VILLEGAS et al., 1997). Therefore, $g(\xi)$ can be written as a Taylor series expansion around one.

Considering in the expansion only the linear contribution, the formulation for $g_{ij}(\xi)$ is:

$$g(\xi) \approx g(1)(3 - 2\xi) \quad (4.13)$$

Galindo et al. (1998) proposed for a square-well potential an expression for the contact value of the radial distribution function for mixtures:

$$g_{ij}^{SW}(1; \zeta_3) = g_{ij}^{HS}(1; \zeta_3) + \beta \varepsilon_{ij} \left[g_{ij}^{HS}(1; \zeta_{3,ij}^{eff}) + (\lambda_{ij}^3 - 1) \left(\frac{\partial g_{ij}^{HS}(1; \zeta_{3,ij}^{eff})}{\partial \zeta_{3,ij}^{eff}} \right) \left(\frac{\lambda_{ij}}{3} \frac{\partial \zeta_{3,ij}^{eff}}{\partial \lambda_{ij}} - \zeta_3 \frac{\partial \zeta_{3,ij}^{eff}}{\partial \zeta_3} \right) \right] \quad (4.14)$$

The contact value of the radial distribution function for the reference system (mixture of hard spheres), at a determined packing fraction, is given by Boublík (1970) as follows:

$$g_{ij}^{HS}(1; \zeta_3) = \frac{1}{1 - \zeta_3} + 3 \frac{D_{ij} \zeta_3}{(1 - \zeta_3)^2} + 2 \frac{(D_{ij} \zeta_3)^2}{(1 - \zeta_3)^3} \quad (4.15)$$

where:

$$\zeta_l = \frac{\pi}{6V} \sum_{i=1}^C N_i m_i \sigma_{ii}^l \quad (4.16)$$

$$D_{ij} = \frac{\sigma_{ii} \sigma_{jj}}{(\sigma_{ii} + \sigma_{jj})} \frac{\zeta_2}{\zeta_3} \quad (4.17)$$

For the calculation of the radial distribution function for the reference system at an effective packing fraction, the following expressions are required:

$$g_{ij}^{\text{HS}}(1; \zeta_3^{\text{eff}}) = \frac{1}{1 - \zeta_3^{\text{eff}}} + 3 \frac{D_{ij} \zeta_3^{\text{eff}}}{(1 - \zeta_3^{\text{eff}})^2} + 2 \frac{(D_{ij} \zeta_3^{\text{eff}})^2}{(1 - \zeta_3^{\text{eff}})^3} \quad (4.18)$$

$$\zeta_{3,ij}^{\text{eff}} = c_1 \zeta_3 + c_2 \zeta_3^2 + c_3 \zeta_3^3 \quad (4.19)$$

$$\begin{bmatrix} c_1 \\ c_2 \\ c_3 \end{bmatrix} = \begin{bmatrix} 2.25855 & -1.50349 & 0.249434 \\ -0.669270 & 1.40049 & -0.827739 \\ 10.1576 & -15.0427 & 5.30827 \end{bmatrix} \times \begin{bmatrix} 1 \\ \lambda_{ij} \\ \lambda_{ij}^2 \end{bmatrix} \quad (4.20)$$

The resulting equation for the calculation of the Helmholtz free energy due to confinement effect is defined as:

$$A^{\text{CONF}} = -N_s \sum_j \sum_i x_{i,s} x_{j,s} \varepsilon_{ij} \Phi_0(3 - 2\xi_{ij}) \left(g_{ij}^{\text{HS}}(\sigma_{ij}; \zeta_3) + \frac{\beta \varepsilon_{ij}}{2} \left(g_{ij}^{\text{HS}}[\sigma_{ij}; \zeta_3^{\text{eff}}] + (\lambda_{ij}^3 - 1) \right. \right. \\ \left. \left. \times \frac{\partial g_{ij}^{\text{HS}}[\sigma_{ij}; \zeta_3^{\text{eff}}]}{\partial \zeta_3^{\text{eff}}} \left(\frac{\lambda_{ij}}{3} \frac{\partial \zeta_3^{\text{eff}}}{\partial \lambda_{ij}} - \zeta_3 \frac{\partial \zeta_3^{\text{eff}}}{\partial \zeta_3} \right) \right) \right) \quad (4.21)$$

4.2 Computational Details

For a complete analytical description of the term A^{CONF} , the next step was to develop an temperature-independent expression for ξ_{ij} . For this purpose, a series of Monte Carlo simulations were performed to obtain the radial distribution function and correlate a temperature-independent expression for ξ_{ij} .

4.2.1 Monte Carlo Simulation

As previously explained, Monte Carlo simulations consist of a very popular simulation tool used to generate a set of representative configurations under specific thermodynamics conditions for a determined system. The main characteristic of this technique is that it is a stochastic approach, where the translation of a molecule is based on random numbers used to analyze whether or not to accept the move, the decision is related to how favorable the energy change would be for states change (FICHTHORN; WEINBERG, 1991).

For the simulations performed in this work, a canonical ensemble was considered, and the initial configuration was settled as a face centered cube. Monte Carlo simulations were carried out for a system with a total of 1372 spherical particles interacting through square-well potential. To the calculation of the potential parameters for dissimilar components, Lorentz-Berthelot combining rules were applied:

$$\sigma_{ij} = \frac{\sigma_{ii} + \sigma_{jj}}{2} \quad (4.22)$$

$$\varepsilon_{ij} = \sqrt{\varepsilon_{ii}\varepsilon_{jj}} \quad (4.23)$$

For the unlike particles attractive range, an arithmetic average was adopted:

$$\lambda_{ij} = \frac{\lambda_{ii} + \lambda_{jj}}{2} \quad (4.24)$$

The Metropolis algorithm was used for each translational attempt, obeying the periodic boundary conditions (ALLEN; TILDESLEY, 2017). The radius of acceptance for this code was set to 0.5 and the equilibration and production steps were 2.744×10^7 each.

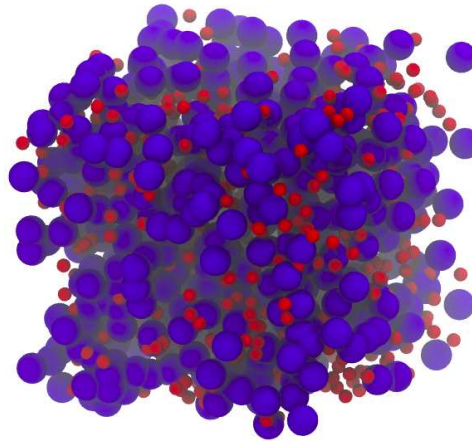


Figure 3 – Snapshot of a Monte Carlo simulation for a binary system.

The position coordinates generated from Monte Carlo Simulation were stored and the radial distribution functions were obtained. Considering a binary system, three radial distribution functions presented in Figure 4 were obtained.

The radial distribution function resulting from simulation was evaluated at the contact, and compared with the predicted value from the equation developed by Gil-Villegas et al. (1998). To search for an accurate value for the radial distribution function at the contact, a quadratic function was fit to the region in the plot where the fluid is attracted to the solid wall, between

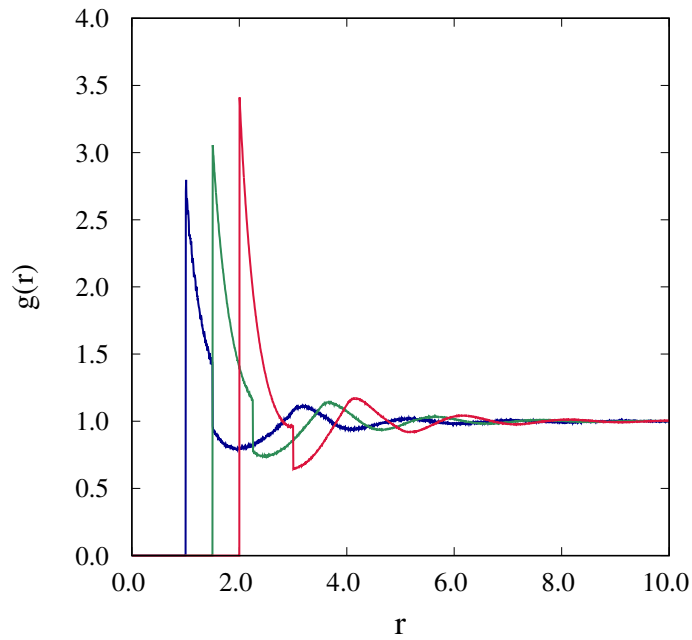


Figure 4 – Radial distribution functions for a mixture with composition 25% – 75%: Blue line is the radial distribution function for the pure component with $\sigma = 1$, red line is the pure component with $\sigma = 2$ and the green line is the radial distribution function for mixture. The range of attraction λ was set to 1.5 for each component

σ and $\lambda\sigma$ (JACKSON; CHAPMAN; GUBBINS, 1988). Based on these points, a curve was adjusted and a more precise value for the radial distribution function at the contact was obtained. The comparison between the value resulting from the simulation and the one obtained from the equation for mixtures with different compositions with equal range of attraction $\lambda = 1.5$, diameters of $\sigma_{11} = 1$ and $\sigma_{22} = 2$ are shown in Figure 5.

The radial distribution function of a pure fluid must satisfy the ideal gas limit relation which establishes that at densities close to zero it must reduce to its ideal gas limit of unity, as shown in Equation 4.25. To emphasize this criterion the y-axis was multiplied by $\exp(-\beta\varepsilon)$. For a better visualization of the behavior of the curves, the green, black and blue curves are shifted on the y-axis of 1, 2 and 3 respectively.

$$\lim_{\eta \rightarrow 0} g(1)e^{-\beta\varepsilon} = 1 \quad (4.25)$$

From Figure 5, one may infer that the expression used to calculate the radial distribution function at contact showed satisfactorily agreement with the simulations. However at low densities, the equation does not satisfy the following ideal gas limit. Since the aim of this work is to study confined fluids systems, the region of interest is the one at high densities which presents a good agreement with the simulations

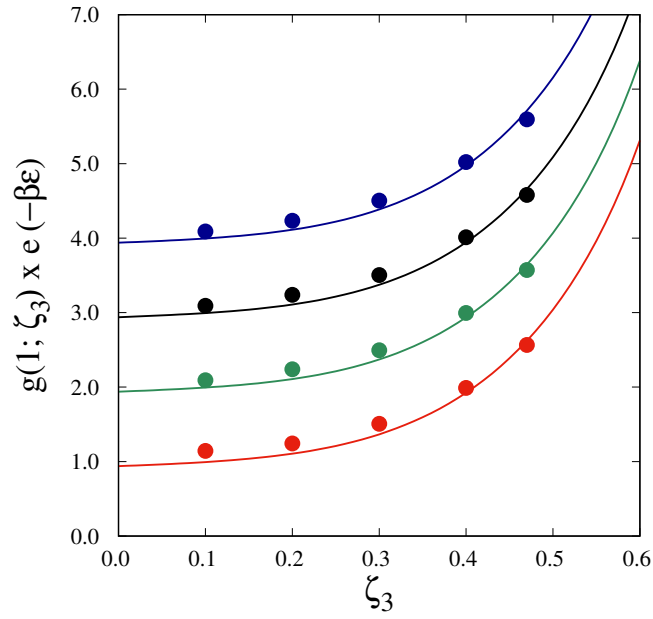


Figure 5 – Radial distribution function at contact for different compositions: blue line = 40%-60%; black line = 25%-75%; green line = 20%-80%; red line = 10%-90%

Isolating ξ_{ij} from Equation 4.13 we have:

$$\xi_{ij} = \frac{1}{2} \left[3 - \frac{g(\xi_{ij})}{g(1)} \right] \quad (4.26)$$

$g_{ij}(\xi_{ij})$ is the mean value of $g_{ij}(x)$ evaluated in the interval between 1 and λ . Therefore, from the calculated radial distribution functions, values for $g_{ij}(\xi_{ij})$ were obtained.

$$g(\xi_{ij}) = \frac{3}{\lambda_{ij}^3 - 1} \int_1^\lambda g_{ij}(x) x^2 dx \quad (4.27)$$

The value of ξ_{ij} for unlike molecules can be calculated by the arithmetic average of the values of ξ_{ij} for pure components:

$$\xi_{ij} = \frac{\xi_{ii} + \xi_{jj}}{2} \quad (4.28)$$

According to Franco, Economou and Castier (2017), the value of ξ_{ii} is well approximated by the following empirical equation fitted to Monte Carlo simulation results:

$$\xi_{ii} = \left(\frac{\lambda_{ii} + 1}{2} \right) + \left(\frac{\lambda_{ii} - 1}{2} \right) \tanh [(\alpha_1 \lambda_{ii} + \beta_1) \zeta_3 + \alpha_2 \lambda_{ii} + \beta_2] \quad (4.29)$$

where $\alpha_1 = -4.3154$, $\alpha_2 = 1.0397$, $\beta_1 = 11.021$, and $\beta_2 = -3.2542$.

Figure 6 shows a quite satisfactory agreement between values of ξ_{12} calculated by Equations (4.28) and (4.29) and by Monte Carlo simulations for different square-well binary mixtures (25% of molecules type 1 and 75% of molecules type 2): i) $\lambda_{11} = 1.1$, $\lambda_{22} = 1.3$, and $\lambda_{12} = 1.2$; ii)

$\lambda_{11} = 1.125$, $\lambda_{22} = 1.500$, and $\lambda_{12} = 1.313$; and iii) $\lambda_{11} = 1.375$, $\lambda_{22} = 1.625$, and $\lambda_{12} = 1.500$. The influences of molecule size and composition are taken into account in ζ_3 .

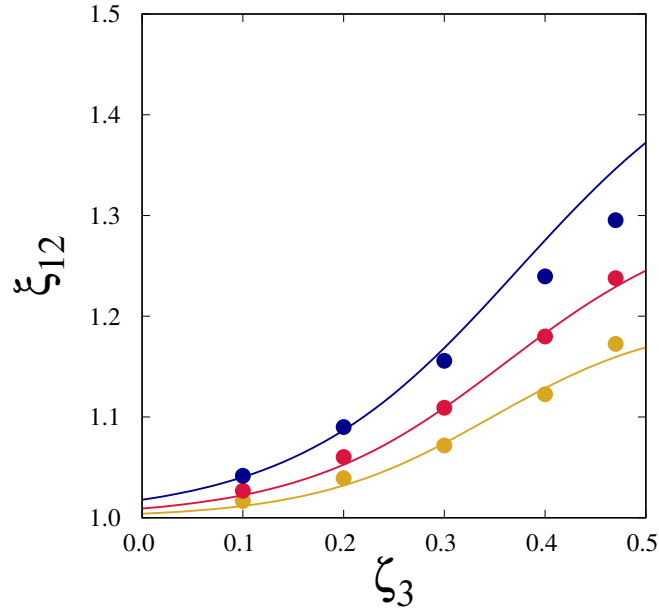


Figure 6 – ξ_{12} as function of ζ_3 for different square-well binary mixtures (25% of molecules type 1 and 75% of molecules type 2): i) $\lambda_{11} = 1.1$, $\lambda_{22} = 1.3$, and $\lambda_{12} = 1.2$ (yellow); ii) $\lambda_{11} = 1.125$, $\lambda_{22} = 1.500$, and $\lambda_{12} = 1.313$ (red); iii) and $\lambda_{11} = 1.375$, $\lambda_{22} = 1.625$, and $\lambda_{12} = 1.500$ (blue); Closed symbols, Monte Carlo simulations. Continuous lines, Equations (4.28) and (4.29).

4.2.2 Phase equilibrium calculations

When the adsorbate is in contact with the adsorbent, the molecules tend to flow from the bulk phase to the adsorbent surface until the chemical potential on the bulk phase equals the adsorbed phase. When the chemical potentials are equal, the system is in equilibrium. Information on the adsorption equilibrium is crucial to understand the adsorption process. The phase equilibrium criteria for adsorption are given by the equality of temperature and the equality of each component chemical potential in both adsorbed and bulk phases:

$$\mu_{i,\text{ads}}(T, V_{\text{ads}}, \mathbf{n}_{\text{ads}}) = \mu_{i,\text{bulk}}(T, p_{\text{bulk}}, \mathbf{n}_{\text{bulk}}) \quad \text{for } i = 1, \dots, C \quad (4.30)$$

where $\mu_{i,\text{ads}}$ is the chemical potential of component i in the adsorbed phase, T is the absolute temperature, V_{ads} is the volume of the adsorbed phase, $\mathbf{n}_{\text{ads}} = [n_{1,\text{ads}}, \dots, n_{C,\text{ads}}]$ contains the amount of each component in the adsorbed phase, $\mu_{i,\text{bulk}}$ is the chemical potential of component i in the bulk phase, p_{bulk} is the bulk pressure, and $\mathbf{n}_{\text{bulk}} = [n_{1,\text{bulk}}, \dots, n_{C,\text{bulk}}]$ contains the amount of each component in the bulk phase.

Once we have a complete description of the Helmholtz free energy, the chemical potential of each component can be calculated by:

$$\mu_i = \left(\frac{\partial A}{\partial n_i} \right)_{T,V,n_{j \neq i}} \quad (4.31)$$

One of the approaches used in modeling phase equilibrium problems is solving a system of nonlinear equations that describe the equilibrium conditions. The solution of these equations must be solved employing an iterative method. The method applied in this work is the multidimensional secant. An outline of this method is presented here.

To solve a system of equations, we need to find a set of values of x that simultaneously equals all the equations to zero.

$$\begin{cases} f_1(x_1 \dots x_n) = 0 \\ \vdots \\ f_n(x_1 \dots x_n) = 0 \end{cases} \quad (4.32)$$

hence, this system can be written as:

$$F(\mathbf{x}) = 0 \quad (4.33)$$

The secant method requires the derivative of a function to estimate the root. This method is basically a modification of the Newton-Raphson method for cases where the evaluation of the derivative of a function is quite costly. Therefore, in this approach the derivative is numerically calculated. The estimation of the root is based on a first-order Taylor series expansion of the multidimensional function F :

$$F(x) = F(x_k) + F'(x_k)(x - x_k) \quad (4.34)$$

where $F'(x_k)$ is the Jacobian matrix $J(x_k)$.

Writing Equation 4.34 in an iterative scheme, we have:

$$x_{k+q} = x_k + \delta_k \quad (4.35)$$

where:

$$\delta_k = -F(x_k)J(x_k)^{-1} \quad (4.36)$$

The multidimensional secant method is now applied to solve the system of non-linear equations expressed by Equation (4.37). To solve this system, we need values of n_{ads} that at a

specified bulk pressure, temperature, and n_{bulk} result in the equality of each component chemical potential in both adsorbed and bulk phases.

$$f_i = \mu_{i,\text{ads}}(T, V_{\text{ads}}, \mathbf{n}_{\text{ads}}) - \mu_{i,\text{bulk}}(T, p_{\text{bulk}}, \mathbf{n}_{\text{bulk}}) = 0 \quad \text{for } i = 1, \dots, C \quad (4.37)$$

hence,

$$\mathbf{n}_{\text{ads}}^{(k+1)} = \mathbf{n}_{\text{ads}}^{(k)} - \mathbf{J}^{-1}(\mathbf{n}_{\text{ads}}^{(k)}) \cdot \mathbf{f}(\mathbf{n}_{\text{ads}}^{(k)}) \quad (4.38)$$

where $\mathbf{f}(\mathbf{n}_{\text{ads}}) = [f_1(\mathbf{n}_{\text{ads}}), \dots, f_C(\mathbf{n}_{\text{ads}})]$, and $\mathbf{J}(\mathbf{n}_{\text{ads}})$ is the Jacobian matrix:

$$\mathbf{J}(\mathbf{n}_{\text{ads}}) = \begin{bmatrix} \frac{\partial \mu_{1,\text{ads}}}{\partial n_{1,\text{ads}}} & \dots & \frac{\partial \mu_{1,\text{ads}}}{\partial n_{C,\text{ads}}} \\ \vdots & \ddots & \vdots \\ \frac{\partial \mu_{C,\text{ads}}}{\partial n_{1,\text{ads}}} & \dots & \frac{\partial \mu_{C,\text{ads}}}{\partial n_{C,\text{ads}}} \end{bmatrix} \quad (4.39)$$

The method developed by Topliss et al. (1988) was used to calculate the bulk volume. Given the calculated volume, the SAFT-VR Mie equation of state was used to calculate the chemical potential of the bulk phase.

The differential elements of the Jacobian are computed numerically. The inverse of a matrix exists if and only if the value of its determinant is equal to zero. The approach used to invert the Jacobian matrix in this work was the Adjoint method.

When J is invertible, then its inverse can be obtained by the formula:

$$J^{-1} = \text{ADJ}(J) \frac{1}{\text{DET}(J)} \quad (4.40)$$

The cofactor of matrix J , C_{ij} , is given by:

$$C_{ij} = (-1)^{i+j} \text{DET}(M_{ij}) \quad (4.41)$$

where M_{ij} is the minor matrix obtained from A removing the i -th row and j -th column. The adjoint of a matrix, $\text{ADJ}(J)$, is calculated as follows:

$$\text{ADJ}(J) = C^T \quad (4.42)$$

The derivatives of the Jacobian matrix were calculated as numerical approximations (forward differentiating):

$$f'(x) \approx \frac{f(x+h) - f(x)}{h} \quad (4.43)$$

where h is a very small number that represents a small change in x .

The convergence criterion for the multidimensional secant method was stipulated as:

$$\sqrt{\sum_{i=1}^C \left(\frac{\mu_{i,\text{ads}}(T, V_{\text{ads}}, \mathbf{n}_{\text{ads}}^{(k)}) - \mu_{i,\text{bulk}}(T, p_{\text{bulk}}, \mathbf{n}_{\text{bulk}})}{\mu_{i,\text{bulk}}(T, p_{\text{bulk}}, \mathbf{n}_{\text{bulk}})} \right)^2} \leq \epsilon = 10^{-5} \quad (4.44)$$

Although this method has been successfully used in this work for equilibrium computations, it presents some practical difficulties. A good initial guess is required, otherwise, the calculations will often diverge. Moreover, the repeated evaluation of the the Jacobian and its inverse is computationally costly.

4.2.3 Pure component fluid-wall interaction parameters

The interaction potential parameters, λ and ε , were fitted to experimental data for pure component adsorption isotherm. The method adopted in this work for this calculation was the Nelder and Mead simplex algorithm (1965), which is used to find a local minimum of the evaluated function.

The major advantage of this algorithm is that it is a derivative-free method that only uses the values of the objective function. The general idea of this method is to compute the objective function at each vertex of the simplex. A process of moving the Simplex is continued until the optimum value of the function is reached (NOCEDAL; WRIGHT, 1999).

To fit the interaction potential parameters, the object function chosen was the Average Absolute Relative Deviation (AARD) of the adsorbed amount. Using experimental adsorbed amount for pure components, the parameters were fitted until Simplex method searched for the AARD minimum value.

$$\text{AARD} = \frac{1}{N_p} \sum_{k=1}^{N_p} \left| \frac{\Gamma_k^{\text{exp}} - \Gamma_k^{\text{calc}}}{\Gamma_k^{\text{exp}}} \right| \quad (4.45)$$

where N_p is the number of data points, Γ^{exp} is the experimental adsorbed amount, and Γ^{calc} is the calculated adsorbed amount, where $\Gamma = \rho_{\text{ads}} v_p$, ρ_{ads} is the adsorbed mixture density, and v_p is the specific pore volume.

5 Results

The developed model was used to perform adsorption equilibrium calculations for different types of systems. To verify the accuracy of the adsorption isotherms calculated using our model, an Average Absolute Relative Deviation (AARD) between the calculated adsorbed amount and the experimental adsorbed amount (Equation 4.45) obtained in the open literature was calculated for binary and ternary mixtures.

Table 1 presents SAFT-VR Mie pure component parameters for fluid-fluid interactions obtained in the literature. The parameters for methane, propane, and ethane were obtained from (LAFITTE et al., 2013), ethylene and nitrogen from (DUFAL et al., 2015), and hydrogen from (NIKOLAIDIS et al., 2018).

5.1 Binary mixtures

Adsorption isotherms for five binary mixtures on MSC5A at 303.15 K were calculated and compared with a set of experimental data from Konno, Shibata and Saito (1985). The specific surface area and pore volume of this adsorbent are respectively of $650 \text{ m}^2 \cdot \text{g}^{-1}$ and $0.56 \text{ mL} \cdot \text{g}^{-1}$. Considering that MSC5A pore geometry is cylindrical, the pore radius was assumed to be 1.72 nm. The values for the fluid-wall interaction parameters (λ_{wf} and ε_{wf}) for methane, ethane, and propane adsorbed in MSC5A at 303.15 are presented in Table 2. These parameters obtained from Franco, Economou, and Castier (2017), were fitted using the SAFT-VR Mie for confined fluids. The pure component wall-fluid interaction parameters for ethylene adsorbed in MSC5A at 303.15 K were fitted to the adsorption isotherm experimental data set from Nakahara, Hirata, and Omori (1974) using Nelder and Mead simplex algorithm. The AARD for ethylene is 0.91%.

Table 1 – Values of SAFT-VR Mie parameters for fluid-fluid interactions.

Component	m	$\sigma / \text{\AA}$	λ_r	λ_a	$(\varepsilon/k_B) / \text{K}$
methane	1.0000	3.7412	12.650	6	153.36
ethane	1.4373	3.7257	12.400	6	206.12
ethylene	1.7972	3.2991	9.6463	6	142.64
propane	1.6845	3.9056	13.006	6	239.89
nitrogen	1.4214	3.1760	9.8749	6	72.438
hydrogen	1.0000	3.1586	7.8130	6	18.355

Table 2 – Values of wall-fluid interaction parameters (λ_{wf} and ε_{wf}) for the extended SAFT-VR Mie for confined fluids for pure methane, ethane, ethylene, and propane adsorbed on MSC5A at 303.15 K.

Component	λ_{wf}	$(\varepsilon_{wf}/k_B) / \text{K}$
methane	1.480	1647.2
ethane	1.434	2016.3
ethylene	1.474	1784.7
propane	1.440	2111.3

The first binary system to be studied was a mixture of methane and ethane at 13.3 kPa and 40.0 kPa. The performance of the model in predicting the adsorption isotherms for each system is represented in Figures 7 and 8 respectively.

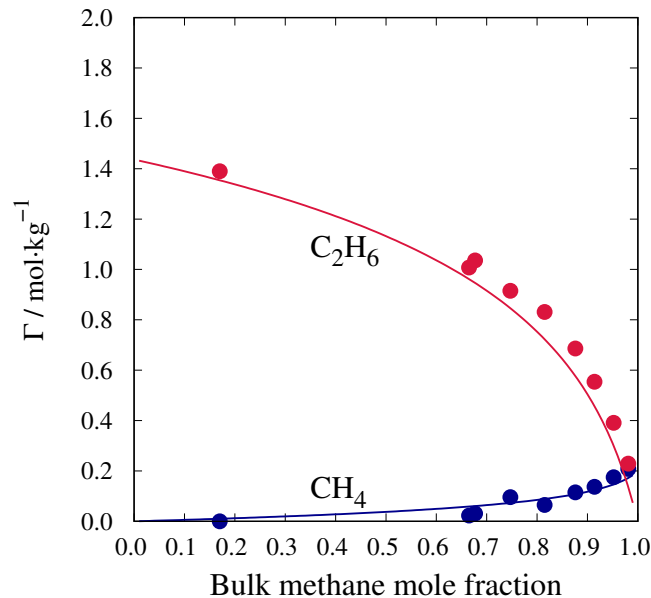


Figure 7 – Adsorption isotherms of methane and ethane on a carbon molecular sieve (MSC5A) at 303.15 K with bulk pressure of 13.3 kPa. Closed symbols, experimental data (KONNO; SHIBATA; SAITO, 1985). Continuous lines, proposed model.

Figures 9 and 10 show the results for the binary mixture ethane-propane adsorbed on MSC5A at 303.15 K with bulk pressures of 13.3 kPa and 40.0 kPa respectively, and Figure 11 shows the adsorption isotherms for ethylene-propane mixture adsorbed on MSC5A at 303.15 K with bulk pressure of 13.3 kPa.

For all the binary systems evaluated on MSC5A, the proposed model satisfactorily predicts the mixture adsorption isotherms. Especially at high bulk pressures, the model tends to better represent the experimental data. In some cases, the model underpredicts the adsorbed amount of the richest component, nevertheless the results calculated using the model always follow

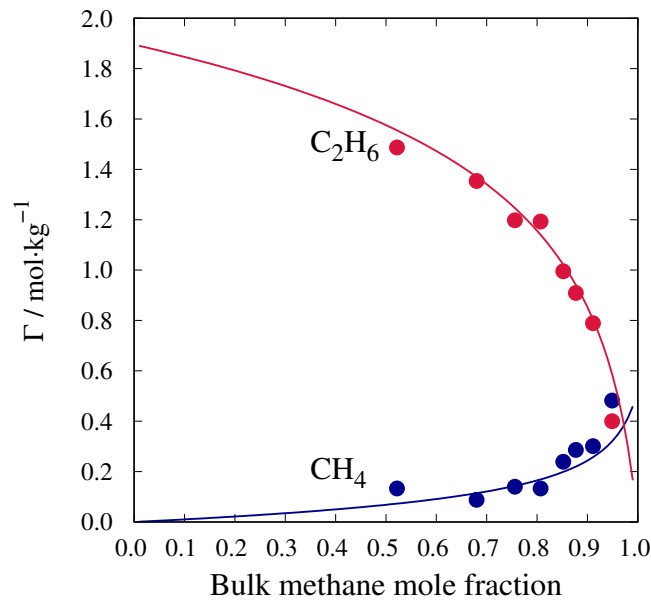


Figure 8 – Adsorption isotherms of methane and ethane on a carbon molecular sieve (MSC5A) at 303.15 K with bulk pressure of 40.0 kPa. Closed symbols, experimental data (KONNO; SHIBATA; SAITO, 1985). Continuous lines, proposed model.

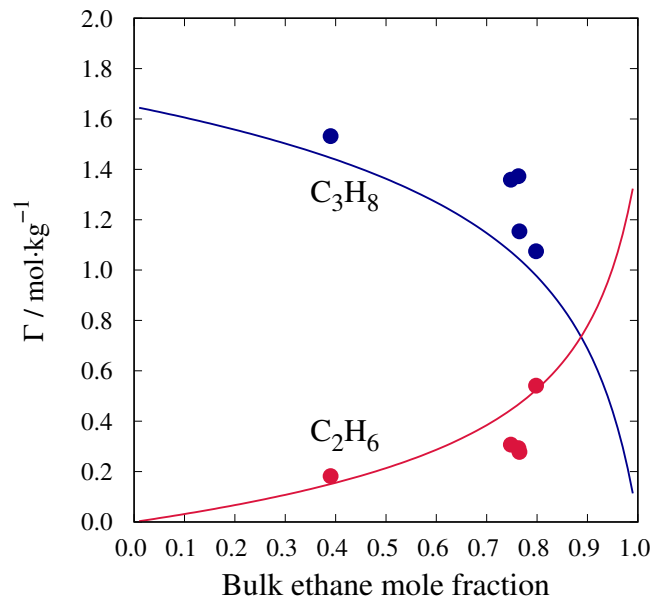


Figure 9 – Adsorption isotherms of ethane and propane on a carbon molecular sieve (MSC5A) at 303.15 K with bulk pressure of 13.3 kPa. Closed symbols, experimental data (KONNO; SHIBATA; SAITO, 1985). Continuous lines, proposed model.

the trend of the experimental data set. In this work, we did not take into account the binary interaction parameters (BIP). BIP's are usually correlated to experimental data of liquid-vapor equilibrium of binary mixtures and are very relevant in the prediction of mixtures by the equation of state. The fitting of these parameters to multicomponent adsorption experimental data might

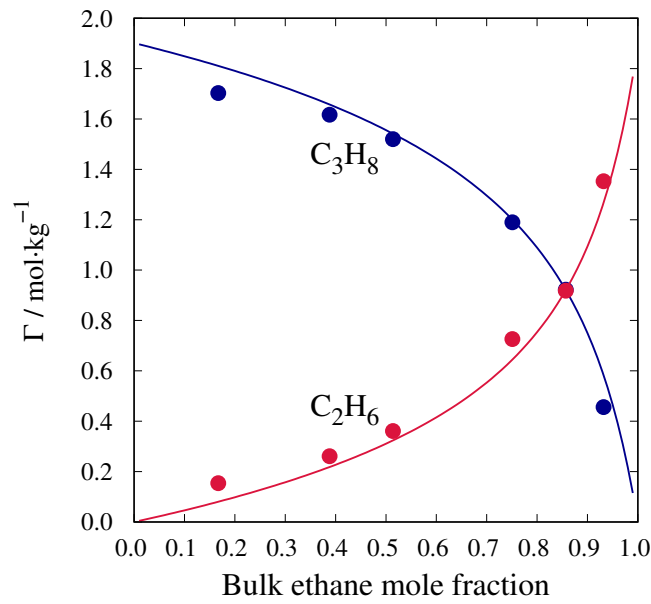


Figure 10 – Adsorption isotherms of ethane and propane on a carbon molecular sieve (MSC5A) at 303.15 K with bulk pressure of 40.0 kPa. Closed symbols, experimental data (KONNO; SHIBATA; SAITO, 1985). Continuous lines, proposed model.

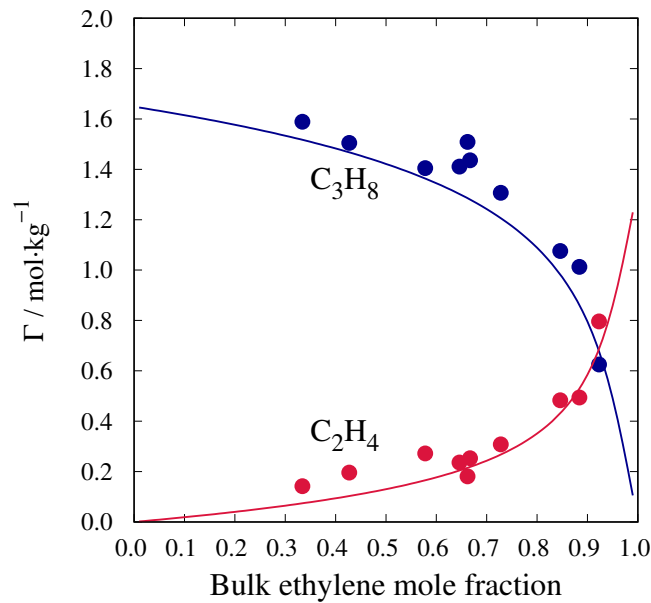


Figure 11 – Adsorption isotherms of ethylene and propane on a carbon molecular sieve (MSC5A) at 303.15 K with bulk pressure of 13.3 kPa. Closed symbols, experimental data (KONNO; SHIBATA; SAITO, 1985). Continuous lines, proposed model.

improve the adsorption isotherm predictions (TRAVALLONI, 2012). For all binary mixtures, the inversion point corresponds to equal composition of both components within the pore is extremely well predicted by the proposed model.

The AARD values between the adsorption isotherms predicted by the proposed model and

the experimental data obtained by (KONNO; SHIBATA; SAITO, 1985) are shown in Table 3. The high AARD values can be justified in some cases due to the low precision of experimental data obtained from literature.

Table 3 – Average Absolute Relative Deviation (AARD) values between the adsorption isotherms predicted by the proposed model and the experimental data obtained by Konno et al. (1985).

$p_{\text{bulk}} / \text{kPa}$	Components	AARD(%)
13.3	methane	45.0
	ethane	16.3
40.0	methane	23.9
	ethane	8.70
13.3	ethane	38.7
	propane	13.8
40.0	ethane	15.3
	propane	6.53
13.3	ethylene	32.0
	propane	6.45

Figure 12 and 13 shows the results for methane-nitrogen mixture adsorbed on MOF-5 at 297.0 K and bulk pressures of 1506 kPa and 502 kPa. MOF-5 is an adsorbent with a spherical shape, thus, considering the specific surface area and the specific pore volume of this adsorbent respectively of $3054 \text{ m}^2 \cdot \text{g}^{-1}$ and $1.31 \text{ cm}^3 \cdot \text{g}^{-1}$ the pore radius is assumed to be 1.28 nm (KLOUTSE et al., 2018). The fluid-wall interaction parameters for pure fluids were fitted using Nelder and Mead simplex method. The values obtained and AARD calculated are summarized in Table 4. Figures 14 and 15 show the adsorption isotherms for pure methane and nitrogen.

Table 4 – Values of wall-fluid interaction parameters (λ_{wf} and ε_{wf}) for the extended SAFT-VR Mie for confined fluids for pure methane and nitrogen adsorbed on MOF-5 at 297 K.

Component	λ_{wf}	$(\varepsilon_{wf}/k_B) / \text{K}$	AARD(%)
methane	1.539	639.082	1.535
nitrogen	1.80	202.262	18.934

For the binary mixtures on MOF-5, the model was also able to predict the adsorption isotherms with reasonable precision. The AARD values calculated for these systems are presented in Table 5. For these cases, the model performance might not just be influenced by the absence of BIP parameters, but also by the bad fitting of nitrogen wall-fluid interaction parameters. Considering that the nitrogen AARD in the binary mixture was also larger than

Table 5 – Average Absolute Relative Deviation (AARD) values between the adsorption isotherms predicted by the proposed model and the experimental data obtained by Kloutse et al. (2018)

$p_{\text{bulk}} / \text{kPa}$	Components	AARD(%)
502.0	methane	15.82
	nitrogen	21.89
1506.0	methane	16.55
	nitrogen	21.87

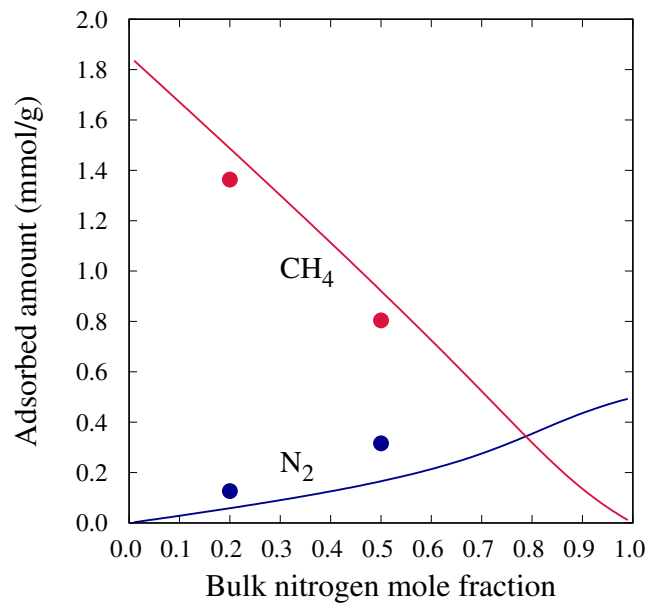


Figure 12 – Adsorption isotherms of methane and nitrogen on a MOF-5 at 297.0 K with bulk pressure of 502.0 kPa. Closed symbols, experimental data (KLOUTSE et al., 2018). Continuous lines, proposed model.

methane, it might suggest that errors in the correlation of the pure fluid interaction parameters might be transmitted to mixtures prediction.

5.1.1 Ternary Mixtures

The ternary mixture composed of methane, nitrogen, and hydrogen on activated carbon JX101 at 313 K and 298 K was also evaluated. The bulk composition was fixed at: 0.3648, 0.2775 and 0.3577 for methane, nitrogen, and hydrogen, respectively. As reported by Wu et al. (2005), the activated carbon was considered to have a surface area of $1500 \text{ m}^2 \cdot \text{g}^{-1}$, and pore volume of $0.52 \text{ mL} \cdot \text{g}^{-1}$. Assuming that activated carbon JX101 have a cylindrical pore, the pore radius calculated was 0.693 nm.

The pure component wall-fluid parameters for the adsorption of methane, nitrogen, and

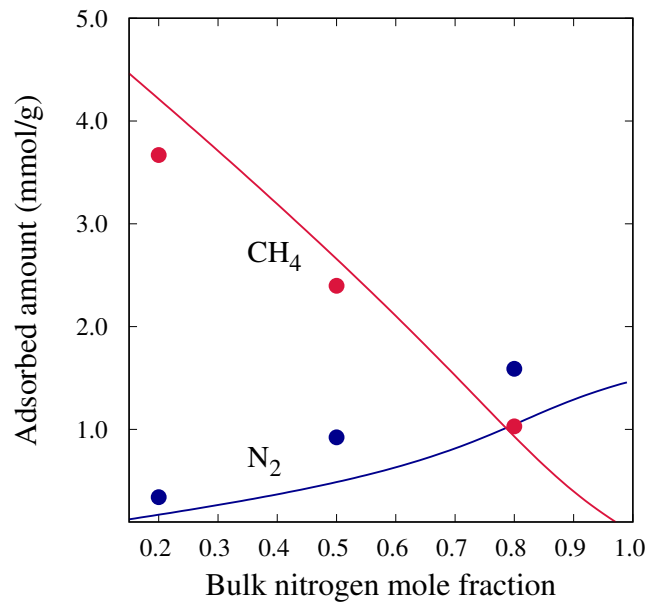


Figure 13 – Adsorption isotherms of methane and nitrogen on a MOF-5 at 297.0 K with bulk pressure of 1506.0 kPa. Closed symbols, experimental data (KLOUTSE et al., 2018). Continuous lines, proposed model.

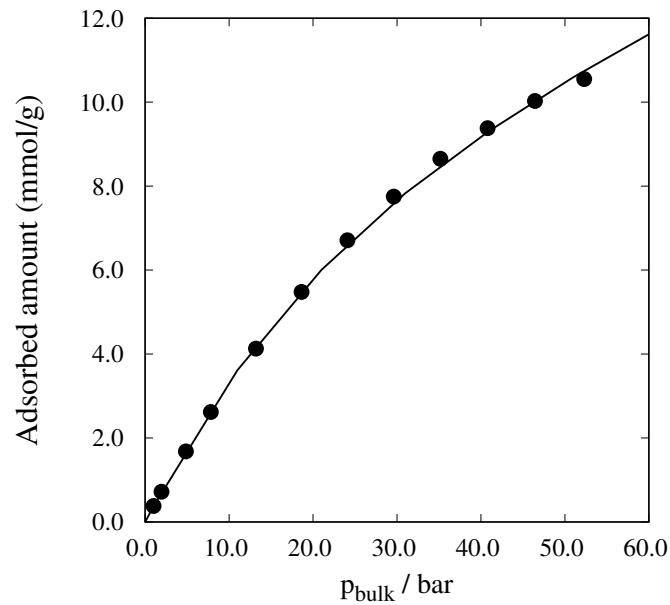


Figure 14 – Adsorption isotherm for pure methane on MOF-5 at 297 K. Closed symbols, experimental data (KLOUTSE et al., 2018). Continuous lines, proposed model.

hydrogen were fitted to the experimental data obtained by Wu et al. (2005), using Nelder and Mead simplex algorithm. All the fitted values, as well as the AARD values, are shown in Table 6. Figures 16 and 17 show the results obtained for correlation of adsorption of pure hydrogen.

Figure 18 and 19 presents the results obtained for the ternary mixture adsorption on activated carbon JX101 at 298 K and 313 K respectively. The model was found to provide good corre-

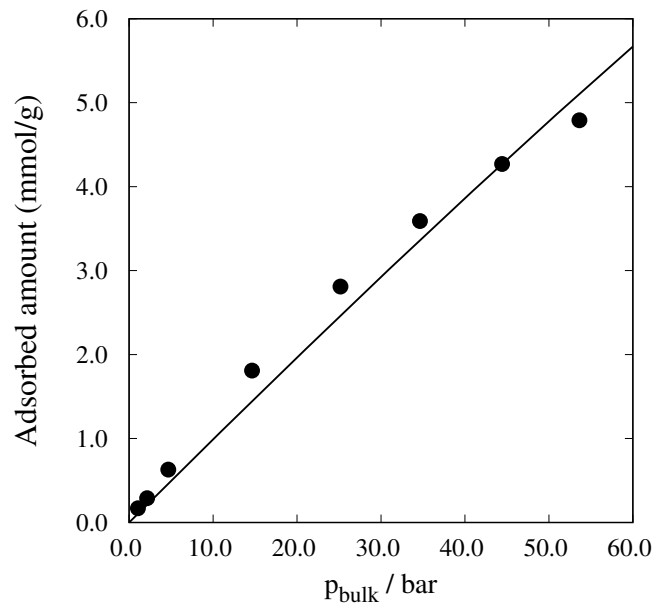


Figure 15 – Adsorption isotherm for pure nitrogen on MOF-5 at 297 K Closed symbols, experimental data (KLOUTSE et al., 2018). Continuous lines, proposed model.

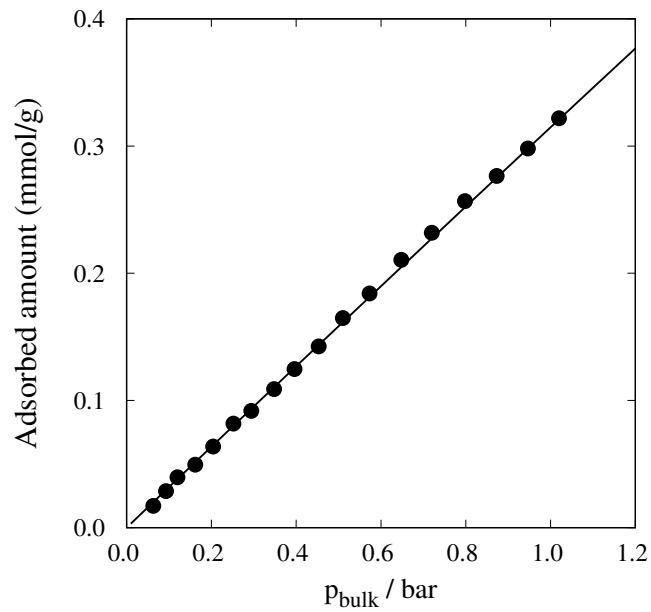


Figure 16 – Adsorption isotherm for pure hydrogen on activated carbon JX101 at 298 K Closed symbols, experimental data (WU et al., 2005). Continuous lines, proposed model.

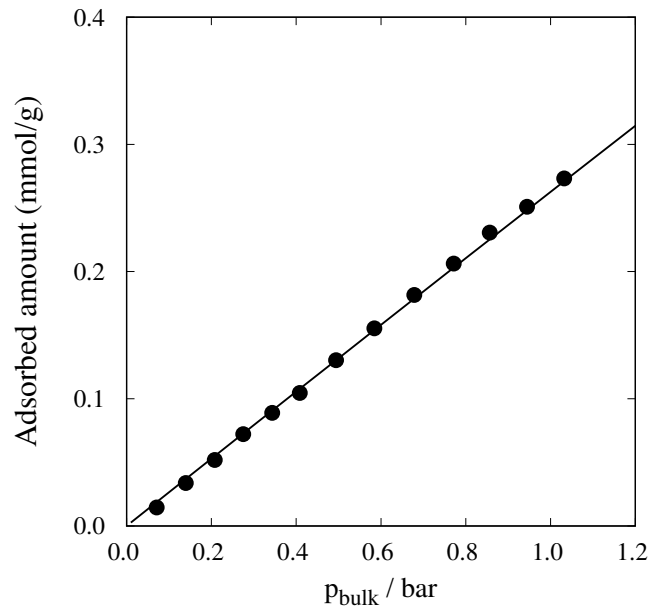


Figure 17 – Adsorption isotherm for pure hydrogen on activated carbon JX101 at 313 K Closed symbols, experimental data (WU et al., 2005). Continuous lines, proposed model.

Table 6 – Values of wall-fluid interaction parameters (λ_{wf} and ε_{wf}) for the extended SAFT-VR Mie for confined fluids for pure methane, nitrogen, and hydrogen adsorbed on JX101 at 298 K and 313 K.

Temperature / K	Component	λ_{wf}	$(\varepsilon_{wf}/k_B) / K$	AARD(%)
313.0	methane	1.425	887.481	1.34
	nitrogen	1.744	482.252	0.93
	hydrogen	1.800	114.251	4.46
298.0	methane	1.289	909.160	2.41
	nitrogen	1.628	511.820	2.49
	hydrogen	1.799	152.070	2.62

Table 7 – Average Absolute Relative Deviation (AARD) values between the adsorption isotherms predicted by the proposed model and the experimental data obtained by Wu et al. (2005).

Temperature / K	Components	AARD(%)
298.0	methane	16.57
	nitrogen	13.63
	hydrogen	72.27
313.0	methane	8.10
	nitrogen	4.34
	hydrogen	71.1

lations for methane and nitrogen, but for hydrogen, the results significantly disagree with the experimental data as shown by the calculated AARD values presented in Table 7. Despite this large deviation, Figure 16 and 17 shows that the model satisfactorily correlated the experimental

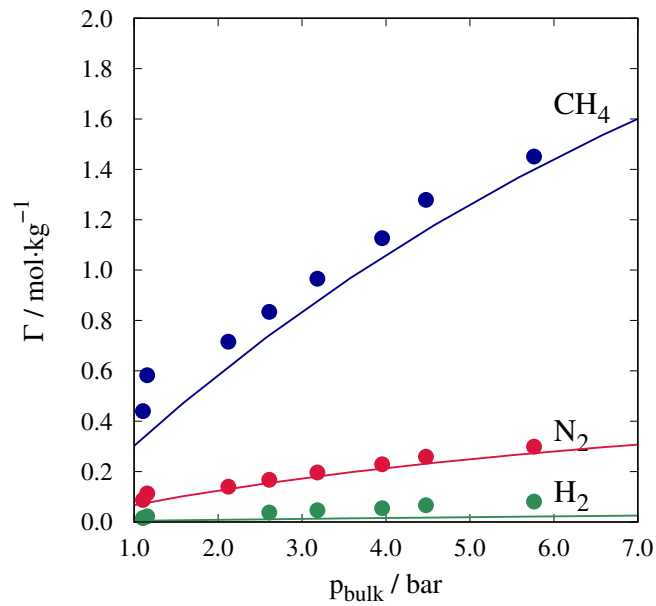


Figure 18 – Adsorption isotherm for the ternary mixture of methane, nitrogen, and hydrogen on activated carbon JX101 at 298 K with bulk mole fractions of 0.3648, 0.2775, and 0.3577, respectively. Closed symbols, experimental data (WU et al., 2005). Continuous lines, proposed model.

data for pure fluid (also see Table 6). Excluded the hypothesis of bad fitting of the fluid-wall interaction parameters used, this quantitative disagreement from the experimental data might be explained by two main reasons. The first is that the unconfined mixture of methane and nitrogen with hydrogen is highly asymmetric, being necessary in some cases the fitting of a temperature-dependent BIP. Second, the quantum description of hydrogen is known to be very relevant for mixtures with large mole fraction of hydrogen (TREJOS; MARTÍNEZ; GIL-VILLEGAS, 2018).

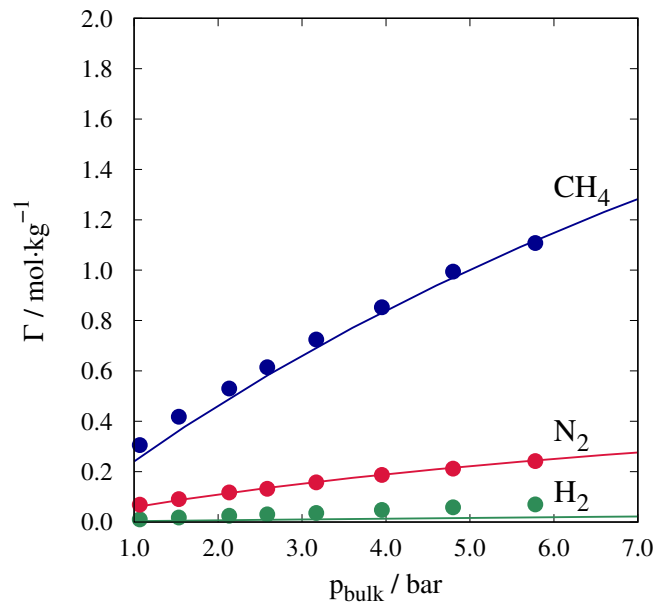


Figure 19 – Adsorption isotherm for the ternary mixture of methane, nitrogen, and hydrogen on activated carbon JX101 at 313 K with bulk mole fractions of 0.3648, 0.2775, and 0.3577, respectively. Closed symbols, experimental data (WU et al., 2005). Continuous lines, proposed model.

6 Conclusions

In this work, the Statistical Associating Fluid Theory (SAFT-VR Mie) was extended to describe confined fluids mixtures. The developed model is a generalization for mixtures of Franco, Economou, and Castier (2017) model, which was derived to correlate pure fluids adsorption isotherms. The theoretical formulation of this approach is based on the generalized van der Waals framework. The fluid-wall interaction was described by the square-well potential, and the structural arrangement for the adsorbed fluid was derived by applying the mean value theorem.

The formulated mathematical expression takes into account the effect of pore size and geometry and the intensity of the interaction between the confining material and the fluid. The predictions of the multicomponent isotherms calculated with our model required no fitting parameters, but only combining rules of the pure fluid-wall interaction parameters previously correlated using pure fluid experimental data set. Moreover, the model can be applied to describe the behavior of fluids in adsorbent with different pore geometries and sizes. The theoretical framework in which this approach is rooted was proved to give good correlation with pure fluids experimental data, and now restate its applicability for multicomponent systems also corresponding experimental data quite well. A strategy to make the model even more general and able to account for the real features of the adsorbent, would be a better description of the fluid structure avoiding the decoupling of fluid-fluid and fluid-wall interactions. The model can also be reformulated to tackle multiple pore sizes, making possible to model adsorbents with large pore size and geometries distribution. Based on existing SAFT approach to deal with electrolytes (GIL-VILLEGAS; GALINDO; JACKSON, 2001) (SELAM; ECONOMOU; CASTIER, 2018), our model can be extended to predict adsorption from electrolyte solutions. The modeling of confined fluids is of practical importance to gas and oil recovery from shale reservoirs. Thus, the comparison of the performance of our proposed EoS with EoS's that do not consider the confinement effect in reservoir simulation remains as good suggestion for future work. Also, the proposed model can be applied to the prediction of mixture adsorption isotherms of associating compounds such as water and alcohols.

Bibliography

- AFRANE, G.; GORDON, P.; GUBBINS, K. E. Experimental investigation of a new supercritical fluid-inorganic membrane separation process. *J. Membr. Sci.*, v. 116, p. 293–299, 1996.
- ALLEN, M. P.; TILDESLEY, D. J. *Computer simulation of liquids*. 2nd. ed. New York: Oxford Science Publications, 2017.
- ARAGUAREN, P. L. . et al. An equation of state for pore-confined fluids. *AIChE J.*, v. 58, p. 3597–3600, 2012.
- ASHOUR, I. et al. Applications of equations of state in the oil and gas industry. In: MORENO, J. C. (Ed.). *Thermodynamics - Kinetics of Dynamic Systems*. Berlin, Heidelberg: InTech, 2011. cap. 7, p. 166–178.
- ASLYAMOV, T.; PLETNEVA, V.; KHLIYUPIN, A. Random surface statistical associating fluid theory: Adsorption of n-alkanes on rough surface. *J. Chem. Phys.*, v. 150, p. 1–11, 2019.
- BALBUENA, P. B.; GUBBINS, E. K. Theoretical interpretation of adsorption behavior of simple fluids in slit pores. *Langmuir*, v. 9, p. 1801–1814, 1993.
- BARBOSA, G. D. et al. Cubic equations of state extended to confined fluids: new mixing rules and extension to spherical pores. *Chem. Eng. Sci.*, v. 153, p. 212–220, 2018.
- BARKER, J. A.; HENDERSON, D. Perturbation theory and Equation of State for fluids. II. A successful Theory of Liquids. *J. Chem. Phys.*, v. 47, p. 4714–4721, 1967.
- BARLETTE, V. E.; FREITAS, L. S. G. . Termodinâmica estatística de líquidos com o método de monte carlo. i. metodologia. *Quim. Nova*, v. 22, p. 254–262, 1999.
- BARSOTTI, E. et al. A review on capillary condensation in nanoporous media: Implications for hydrocarbon recovery from tight reservoirs. *Fuel*, v. 184, p. 344–361, 2016.
- BOUBLÍK, T. Hard-sphere equation of state. *J. Chem. Phys.*, v. 53, p. 471–472, 1970.
- BUTZ, J.; ZIMMERMANN, P.; ENDERS, S. Impact of the equation of state on calculated adsorption isotherm using DFT. *J. Chem. Phys.*, v. 109, p. 5596–5606, 1998.
- CARNAHAN, N. F.; STARLING, K. E. Equation of state for nonattracting rigid spheres. *J. Chem. Phys.*, v. 51, p. 635–636, 1969.
- CHAPMAN, W. G. et al. SAFT: Equation-of-state solution model for associating fluids. *Fluid Phase Equilibr.*, v. 52, p. 31–38, 1989.
- CHIOU, C. T. *Partition and Adsorption of Organic Contaminants in Environmental Systems*. New York: John Wiley Sons, Inc., 2002.
- CRACKNELL, R. F.; CHIMOWITZ, E. H. Influence of pore geometry on the design of microporous materials for methane storage. *J. Chem. Phys.*, v. 97, p. 494–499, 1993.
- DRABOWISKI, A. Adsorption - from theory to practice. *Adv. Colloid. Interfac.*, v. 93, p. 135–224, 2001.

- DUFAL, S. et al. Developing intermolecular-potential models for use with the SAFT-VR Mie equation of state. *AIChE J.*, v. 61, p. 2891–2911, 2015.
- EARL, D. J.; DEEM, M. W. *Molecular Modeling of Proteins*. New York: Humana Press., 2008.
- ECONOMOU, I. G. Statistical associating fluid theory: A successful model for the calculation of thermodynamic and phase equilibrium properties of complex fluid mixtures. *Ind. Eng. Chem. Res.*, v. 41, p. 953–962, 2002.
- FICHTHORN, A. K.; WEINBERG, W. H. Theoretical foundations of dynamical Monte Carlo simulations. *J. Chem. Phys.*, v. 93, p. 1090–1096, 1991.
- FRANCO, L. F. M.; ECONOMOU, I. G.; CASTIER, M. Statistical mechanical model for adsorption coupled with SAFT-VR Mie equation of state. *Langmuir*, v. 33, p. 11291–11298, 2017.
- GALINDO, A. et al. The thermodynamics of mixtures and the corresponding mixing rules in the saft-vr approach for potentials of variable range. *Mol. Phys.*, v. 93, p. 241–252, 1998.
- GELB, D. L. et al. Phase separation in confined systems. *Rep. Prog. Phys.*, v. 62, p. 1573–1659, 1999.
- GIL-VILLEGAS, A.; GALINDO, A.; JACKSON, G. A statistical associating fluid theory for electrolyte solutions (SAFT-VRE). *Mol. Phys.*, v. 99, p. 531–546, 2001.
- GIL-VILLEGAS, A. et al. Statistical associating fluid theory for chain molecules with attractive potentials of variable range. *J. Chem. Phys.*, v. 106, p. 4168–4186, 1997.
- GROSS, J.; SADOWSKI, G. Perturbed-chain saft: an equation of state based on a perturbation theory for chain molecules. *Ind. Eng. Chem. Res.*, v. 40, p. 1244–1260, 2001.
- JACKSON, G.; CHAPMAN, W. G.; GUBBINS, K. E. Phase equilibria of associating fluids of spherical and chain molecules. *Int. J. Thermophys.*, v. 9, p. 769–779, 1988.
- JAYANT, K. S.; SANG, K. K. Surface tension and vapor-liquid phase coexistence of confined square-well fluid. *J. Chem. Phys.*, v. 126, p. 1–8, 2007.
- KELLER, J.; STAUDT, R. *Gas Adsorption Equilibria : Experimental Methods and Adsorptive Isotherms*. Boston, MA: Springer., 2005.
- KIM, H. et al. Thermodynamics of d-dimensional hard sphere fluids confined to micropores . *J. Chem. Phys.*, v. 134, p. 1–12, 2011.
- KLEINER, M.; TUMAKAKA, F.; SADOWSKI, G. Thermodynamic modeling of complex systems. In: LU, J.; HU, Y. (Ed.). *Molecular Thermodynamics of Complex Systems*. Berlin, Heidelberg: Springer, 2009. cap. 2, p. 76–108.
- KLOUTSE, F. A. et al. Experimental benchmark data of ch 4 , co 2 and n 2 binary and ternary mixtures adsorption on mof-5. *Sep. Purif. Technol.*, v. 197, p. 228–236, 2018.
- KONNO, M.; SHIBATA, K.; SAITO, S. Adsorption of light hydrocarbon mixtures on molecular sieving carbon MSC-5A. *J. Chem. Eng. Jpn.*, v. 18, p. 394–398, 1985.
- LAFITTE, T. et al. Accurate statistical associating fluid theory for chain molecules from Mie segments. *J. Chem. Phys.*, v. 139, p. 154504, 2013.

- MARTINEZ, A.; TREJOS, V. M.; GILL-VILLEGAS, A. Predicting adsorption isotherms for methanol and water onto different surfaces using the soft-vr-2d approach and molecular simulation. *Adsorption.*, v. 449, p. 207e216, 2017.
- MCCABE, W. L.; SMITH, J. C.; HARRIOT, P. *Unit Operations Of Chemical Engineering*. New York: McGraw-Hill Education, 1993.
- MCQUARRIE, D. A. *Statistical mechanics*. Sausalito: University Science Books, 2000.
- MYERS, A. L.; PRAUSNITZ, J. M. Thermodynamics of mixed-gas adsorption. *AIChE J.*, v. 11, p. 121–127, 1965.
- NAKAHARA, T.; HIRATA, M.; OMORI, T. Adsorption of hydrocarbons on carbon molecular sieve. *J. Chem. Eng. Data*, v. 19, p. 310–313, 1974.
- NASCIMENTO, R. F. et al. *Adsorção: Aspectos teóricos e aplicações ambientais*. Brasil: Imprensa Universitária da Universidade Federal do Ceará (UFC), 2014.
- NELDER, J.; MEAD, R. A simplex method for function minimization. *Comp. J.*, v. 7, p. 308–313, 1965.
- NIKOLAIDIS, I. K. et al. Modeling of physical properties and vapor-liquid equilibrium of ethylene and ethylene mixtures with equations of state. *Fluid Phase Equilibr.*, v. 470, p. 149–163, 2018.
- NOCEDAL, J.; WRIGHT, S. J. *Numerical Optimization*. New York: Springer, 1999.
- PENG, D.-Y.; ROBINSON, D. B. A new two-constant equation of state. *Ind. Eng. Chem. Fundam.*, v. 15, p. 59–64, 1976.
- PRAUSNITZ, J. M.; LICHTENTHALER, L. M.; AZEVEDO, E. G. *Molecular thermodynamics of fluid-phase equilibria*. New Jersey: Prentice Hall., 1999.
- ROMANIELO, L. L. *Modelagem matemática e termodinâmica da adsorção gasosa*. 240 p. Tese (Doutorado) — Universidade Estadual de Campinas, Campinas, 1999.
- SANDLER, S. I. The generalized van der Waals partition function. I. Basic theory. *Fluid Phase Equilibr.*, v. 19, p. 233–257, 1985.
- SELAM, M. A.; ECONOMOU, I. G.; CASTIER, M. A thermodynamic model for strong aqueous electrolytes based on the eSAFT-VR Mie equation of state. *Fluid Phase Equilibr.*, v. 464, p. 47–63, 2018.
- SOAVE, G. Equilibrium constants from a modified redlich-kwong equation of state. *Chem. Eng. Sci.*, v. 27, p. 1197–1203, 1972.
- TOLEDO, B. I. et al. Bisphenol a removal from water by activated carbon. Effects of carbon characteristics and solution chemistry. *Environ. Sci. Technol.*, v. 39, p. 6246–6250, 2005.
- TOPLISS, R. J.; DIMITRELIS, D.; PRAUSNITZ, J. M. Computational aspects of a non-cubic Equation of State for phase equilibrium calculations: Effect of density-dependent mixing rules. *Comput. Chem. Eng.*, v. 12, p. 483–489, 1988.
- TRAVALLONI, L. *Desenvolvimento de Equaçãode Estado Para Fluidos Confinados*. 86 p. Tese (Doutorado) — Universidade Federal do Rio de Janeiro, Rio de Janeiro, 2012.

TRAVALLONI, L.; CASTIER, M.; TAVARES, F. W. Phase equilibrium of fluids confined in porous media from an extended Peng-Robinson equation of state. *Fluid Phase Equilib.*, v. 362, p. 335–341, 2014.

TRAVALLONI, L. et al. Thermodynamic modeling of confined fluids using an extension of the generalized van der Waals theory. *Chem. Eng. Sci.*, v. 65, p. 3088–3099, 2010.

TREJOS, V. M.; MARTÍNEZ, A.; GIL-VILLEGAS, A. Semiclassical SAFT-VR 2D modeling of adsorption selectivities for binary mixtures of hydrogen and methane adsorbed on MOFs. *Fluid Phase Equilib.*, v. 462, p. 153–171, 2018.

WALTON, K. S.; SHOLL, D. S. Predicting multicomponent adsorption: 50 years of the ideal adsorbed solution theory. *AIChE J.*, v. 61, p. 2757–2762, 2015.

WU, K. et al. Adsorption equilibrium of the mixture $\text{CH}_4+\text{N}_2+\text{H}_2$ on activated carbon. *J. Chem. Eng. Data*, v. 50, p. 635–642, 2005.

ZARRAGOIOCOECHEA, G. J.; KUZ, A. V. van der waals equation of state for a fluid in a nanopore. *J. Chem. Phys.*, v. 65, p. 1–4, 2002.

ZARRAGOIOCOECHEA, G. J.; KUZ, A. V. Critical shift of a confined fluid in a nanopore. *Fluid Phase Equilib.*, v. 220, p. 1–9, 2004.

ZHANG, J.; TODD, B. D.; TRAVIS, K. P. Viscosity of confined inhomogeneous nonequilibrium fluids. *J. Chem. Phys.*, v. 121, p. 10778–10786, 2004.